Stochastic Modeling for Palm Biomass Supply Chain

Bing Shen How, Shirleen Lee Yuen Lo, Karen Gah Hie Kong, and Sin Yong Teng

Abstract Oil palm industry is one of the key contributors to the Gross Domestic Product (GDP) and Comprehensive National Strength (CNS) of Malaysia. According to the Department of Statistical Malaysia (2021), oil palm industries had contributed about 2.7% or RM 38.26 billion (equivalent to 9.45 billion USD) to Malaysia's GDP in 2019. An abundant amount of palm-based biomass has been generated through oil palm harvesting and palm oil production. Therefore, conceptual design and modeling of the *palm biomass supply chain* are deemed necessary to ensure the sustainability of the oil palm industry. Nevertheless, to enhance the model reliability and robustness, *stochastic modeling* should be opted to incorporate various uncertainties into the supply chain model. Keeping this in mind, this chapter presents an overview of the key supply chain uncertainties that should be incorporated into the supply chain model. It is followed by three illustrative examples which cover (i) biomass selection decision, (ii) facility location decision, and (iii) policy selection decision.

Keywords Biomass supply chain · Uncertainty · Stochastic modeling · Decision-making · Monte Carlo

B. S. How (✉) · S. L. Y. Lo · K. G. H. Kong
Biomass Waste-to-Wealth Special Interest Group, Research Centre for Sustainable Technologies, Faculty of Engineering, Computing and Science, Swinburne University of Technology, Jalan Simpang Tiga, 93350 Kuching, Sarawak, Malaysia
e-mail: bshow@swinburne.edu.my

S. Y. Teng
Institute for Molecules and Materials, Radboud University, P.O. Box 9010, 6500 GL Nijmegen, The Netherlands
e-mail: sinyong.teng@ru.nl

D. C. Y. Foo et al. (eds.), *Sustainable Technologies for the Oil Palm Industry*,
https://doi.org/10.1007/978-981-19-4847-3_6

Nomenclature

Abbreviations

AP	Action plan
AP-1	Engage in demand contract
AP2-HS	Engage in supply contract
AP3-FI	Introduce new financing incentive
AP4-SF	Substitute fossil fuel with biodiesel
AP5-TI	Introduce new tax incentive
AP6-RF	Revise Feed-in-Tariff (FiT) rate
AP7-CM	Introduce carbon management system
BOTA	Bottleneck Tree Analysis
CAPEX	Capital expenditure
CNS	Comprehensive National Strength
DoE	Design of Experiment
EFB	Empty fruit bunch
FiT	Feed-in-tariff
GDP	Gross domestic product
GTFS	Green Technology Financing Scheme
LNG	Liquefied natural gas
MF	Mesocarp fiber
MILP	Mixed Integer Linear Programming
NPV	Net present value
OPEX	Operating expenditure
PBP	Payback Period
PCA	Principal component analysis
PKS	Palm kernel shell

Indices

g	Index for synthetic gas products
m	Index for months
t	Index for years
u	Index of units

Parameters

$\text{Biomass}_{m,t}^{\text{AVAILABLE}}$	Biomass availability at month m in year t (t)

$\text{Biomass}_{\text{EFB}}^{\text{QUALITY}}$	Biomass quality for EFB
$\text{Biomass}_{\text{PKS}}^{\text{QUALITY}}$	Biomass quality for PKS
$\text{Biomass}_{\text{MF}}^{\text{QUALITY}}$	Biomass quality for MF
c	Specific heat capacity of water (J kg/K)
$\text{Cap}^{\text{TRUCK}}$	Vehicle load limit (t)
$C_{m,t}^{\text{BIOMASS}}$	Unit cost of biomass at month m in year t (USD/t)
C_{t}^{BIOMASS}	Unit cost of biomass in year t (USD/t)
C_{u}^{CAPEX}	Capital cost for unit u (USD)
C^{CAPEX}	Total capital cost for the conversion process (USD)
$C_{m,t}^{\text{COAL}}$	Unit cost of coal at month m in year t (USD/t)
C_{t}^{COAL}	Unit cost of coal in year t (USD/t)
C^{CO2}	Compensation cost required per unit of carbon emission (USD/kg)
C^{ELEC}	Unit cost of imported power (USD/kWh)
C^{FIT}	Feed-in-tariff (USD/kWh)
$C_{m,t}^{\text{FUEL}}$	Fuel price at month m in year t (USD/L)
C_{t}^{FUEL}	Fuel price in year t (USD/L)
$C_{u,m,t}^{\text{OPEX}}$	Operating cost for unit u at month m in year t (USD)
C_{t}^{OPEX}	Total operating cost for the conversion process in year t (USD)
$C_{m,t}^{\text{OIL}}$	Bio-oil price at month m in year t (USD/L)
$\text{Cap}^{\text{TRUCK}}$	Vehicle load limit (t)
d^{D}	Distance between polygeneration plant and the demand point (km)
d^{S}	Distance between biomass supply and the polygeneration plant (km)
$\text{Elec}_{m,t}^{\text{REQ}}$	Power demand at month m in year t (kWh)
$F_{m,t}^{\text{OIL\_DEMAND}}$	Bio-oil demand at month m in year t (L)
HV^{coal}	Heating value of coal (MJ/kg)
in	Discount rate (%)
ITA	Tax exemption indicator (USD)
LHV_{g}	Low heating value of gas g (kJ/mol)
LHV^{CHAR}	Low heating value of biochar (MJ/kg)
LHV^{COAL}	Low heating value of coal (MJ/kg)
$\text{MC}_{m,t}^{\text{IN}}$	Moisture content of biomass before drying (%)
$\text{MC}_{t}^{\text{IN}}$	Moisture content of biomass before drying (wt%)
MC^{OUT}	Moisture content of biomass after drying (%)
Q^{FC}	Weight composition of fixed carbon of biomass (wt%)
Q^{VM}	Weight composition of volatile matter of biomass (wt%)
Q^{A}	Weight composition of ash of biomass (wt%)
Q^{MC}	Weight composition of moisture content of biomass (wt%)
Q^{H}	Weight composition of hydrogen of biomass (wt%)
Q^{C}	Weight composition of carbon of biomass (wt%)
Q^{O}	Weight composition of oxygen of biomass (wt%)
Q^{S}	Weight composition of sulfur of biomass (wt%)

Q^{N}	Weight composition of nitrogen of biomass (wt%)
TAX	Corporate tax rate (%)
$\text{Thermal}_{m,t}^{\text{REQ}}$	Heat demand at month *m* in year *t* (kWh)
y^{CHAR}	Biochar yield (%)
$y^{\text{CO2\_COGEN}}$	CO_2 emitted during co-generation unit (kg CO_2/kWh)
$y^{\text{CO2\_PY}}$	CO_2 emitted during pyrolysis process (kg CO_2/kg biomass)
$y^{\text{CO2\_TR}}$	CO_2 emitted during transportation (kg CO_2/L fuel)
y^{GAS}	Syngas yield (%)
y_{g}^{PY}	Molecular composition of gas *g* (%)
y^{OIL}	Bio-oil yield (%)
ξ^{COGEN}	Conversion efficiency of the co-generation unit (%)
ξ^{DRY}	Drying efficiency (%)
ψ^{FUEL}	Fuel consumption rate (L/km)
ψ^{PY}	Thermal energy required to try per unit mass of biomass (kWh/t)
ψ^{THERMAL}	Thermal energy required to try per unit mass of moisture (kWh/t)

Variables

$\text{Biomass}_{m,t}^{\text{DRY}}$	Flowrate of dried biomass fed into the pyrolyser at month *m* in year *t* (t)
$\text{Biomass}_{m,t}^{IN}$	Flowrate of biomass fed into the plant at month *m* in year *t* (t)
$\text{Biomass}_{t}^{\text{IN}}$	Flowrate of biomass fed into the plant in year *t* (t)
$\text{Biomass}_{t}^{\text{SUPPLY}}$	Biomass supply in year *t* (t)
$C_{m,t}^{\text{PENALTY}}$	Carbon penalty at month *m* in year *t* (USD)
$C_{m,t}^{\text{PROCURE}}$	Procurement cost at month *m* in year *t* (USD)
C_{t}^{PROCURE}	Procurement cost in year *t* (USD)
C_{t}^{SYNGAS}	The selling price of syngas in year *t* (USD)
$C_{m,t}^{\text{TR}}$	Transportation cost at month *m* in year *t* (USD)
C_{t}^{TR}	Transportation cost in year *t* (USD)
$CF_{m,t}^{\text{IN}}$	Input cash flow (USD)
CF_{t}^{IN}	Input cash flow in year *t* (USD)
$CF_{m,t}^{\text{OUT}}$	Output cash flow (USD)
CF_{t}^{OUT}	Output cash flow in year *t* (USD)
$\text{Elec}_{m,t}^{\text{EXP}}$	Exported power at month *m* in year *t* (kWh)
$\text{Elec}_{m,t}^{\text{GEN}}$	Generated power at month *m* in year *t* (kWh)
$\text{Elec}_{m,t}^{\text{IMP}}$	Imported power at month *m* in year *t* (kWh)
$F_{m,t}^{\text{CHAR}}$	Biochar production at month *m* in year *t* (t)
$F_{m,t}^{\text{COAL}}$	Coal consumption at month *m* in year *t* (t)
F_{t}^{COAL}	Coal consumption in year *t* (t)
$F_{m,t}^{\text{GAS}}$	Syngas production at month *m* in year *t* (t)

$F_{m,t}^{\mathrm{OIL}}$	Bio-oil production at month m in year t (L)
F_{t}^{SYNGAS}	Syngas demand in year t (MWth)
Q^{coal}	Energy required to reduce the moisture content of biomass (MJ)
S^{BIOMASS}	Specific syngas yield (kg/kg)
T_{Final}	Temperature of biomass after drying (°C)
T_{Initial}	Temperature of biomass before drying (°C)
$\mathrm{NCF}_{m,t}$	Net cash flow at month m in year t (USD)
NCF_{t}	Net cash flow in year t (USD)
$\mathrm{Thermal}_{m,t}^{\mathrm{GEN}}$	Generated heat at month m in year t (kWh)

1 Introduction

Laying the agriculture foundation in Malaysia, the cultivation of the oil palm industry has been emerging ever since the first commercial planting was materialized in Tennamaran Estate, Selangor, in 1917 (The Oil Palm, 2021). Oil palm plantation was first introduced by the Malaysian government to diversify the country's agricultural products and at the same time diminish the nation's economic dependency on rubber and tins in the early 1960s (The Oil Palm, 2021).

Over the years, Malaysia has been showered and fueled with oil palm biomass resulted as the world's second-largest palm oil producer (around 19.14 million tonnes of crude palm oil produced in 2020) (Malaysia Palm Oil Board, 2020). Oil palm biomass exists as one of the most appealing substituents for energy generation feedstock whereas many nations are still exploring diversifying the country's energy profile. In order to appeal to more potential investors into biomass-based industries, a sustainable biomass supply chain (from harvesting to distribution) is required to be systemized and well-ordered. To this end, Hong et al. (2016) had proposed four critical elements in developing a sustainable biomass supply chain, which consists of (i) biomass harvesting and management, (ii) integrated biorefinery, (iii) product distribution, and (iv) logistics management. Nonetheless, Lo et al. (2021) stated that almost 95% of the researchers used deterministic models (Mixed Integer Linear Programming (MILP)) in evaluating biomass supply chain models. However, various uncertainties related to the biomass supply chain are yet to be considered in most of the supply chain optimization models. The relevant works mainly utilize deterministic optimization options in performing their studies and the outcomes may be too ideal which are not realistic in real life. For instance, Zakaria et al. (2020) did mention that deterministic optimization models would opt to generate ideal results which some of the systems are often uncertain in real life, causing the generated results to be impractical and imprecise. The addition of uncertainties and risk parameters into the supply chain model may shift it from deterministic to stochastic, where the model robustness can be enhanced and the outcomes can be more accurate and reliable. Stochastic optimization models with uncertainties integrated are able to develop random-probability-based distribution results (Kieffer et al., 2016), in which the generated outcomes would be more solid (Zakaria et al., 2020). One acknowledged example is the work conducted by Kristianto and Zhu (2017), where the stochastic optimization is implemented in the biomass-to-bioethanol supply chain model, had successfully generated promising results in minimizing emission, energy, and water utilization.

Hence, this chapter focus on four key components as the uncertainty variables to be considered in the stochastic biomass supply chain model:

(i) Biomass quality
(ii) Biomass supply uncertainties
(iii) Biomass demand variation
(iv) Pricing fluctuation.

Considering uncertainties in supply-chain, optimization models may be able to perform probability-based distribution outcomes in which the results might be closer to the real-world scenarios. Though, the details of the uncertainties need to be further discussed to prevent unexpected consequences that would lead to process failure or profit loss. A schematic figure of the basic idea for the uncertainties to be considered in stochastic biomass supply chain optimization models is shown in Fig. 1. The manipulating variables are then demonstrated with three different case scenarios, where the formulated models and their corresponding impacts are further discussed in the later sections.

One of the concerns in developing a sustainable supply chain would be the biomass source of supply (i.e., biomass availability). Various research works were reported to include biomass supply as one of the uncertainties in the biomass supply chain due to different harvesting seasons and logistics arrangements as described by Martinkus et al. (2018) and Lim et al. (2019). In the case of biomass shortage, imported biomass is mandatory, where additional operating costs (transportation cost and importing cost) may be required, which directly affects the profitability and efficiency of the biomass supply chain. Extended from that, various biomass qualities (or characteristics) should also be incorporated into the stochastic biomass supply chain model. It has been reported that the quality of the biomass is the most sensitive parameter

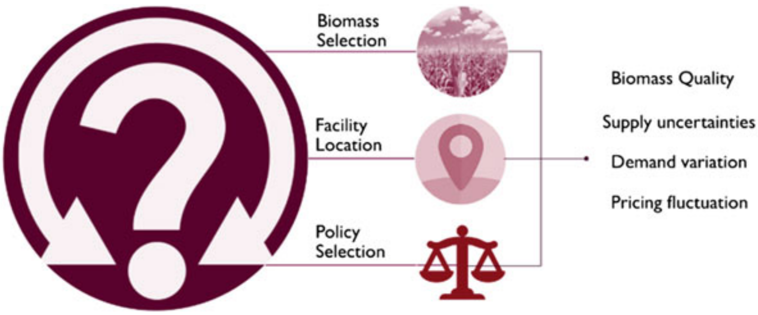

Fig. 1 Key uncertainties considered in stochastic biomass supply chain

in influencing the biorefinery economics, where it has been justified by Baral et al. (2019) that better biomass quality eventually contributes to higher profitability even though higher purchase cost for biomass is required. Another example from How et al. (2019), proved that higher moisture content and low density of biomass quality requires higher logistics cost which increases the prime cost of the biomass and the overall biomass supply chain.

Likewise, the distinctive quality of biomass has a significant impact on their respective conversion routes (e.g. gasification, pyrolysis, anaerobic digestion, etc.). Lim et al. (2019) found that a broader quality range of biomass will lead to higher fluctuation of conversion efficiency. Several research works have discussed the impact of biomass quality on the overall economic feasibility of the biomass supply chain (Bussemaker et al., 2017; Tanzer et al., 2019). For example, the lowering of moisture content of biomass (60% to 40%) would help in reducing the drying cost along with the logistics cost. Similarly, biomass with different compositions would favor the generation of different end products (biochar, bio-oil, etc.), given the various decomposition rate of the respective components (Bussemaker et al. (2017). Hence, the uncertainty of biomass quality plays a crucial role in developing a feasible biomass supply chain.

The quality of biomass not only influences the choice of conversion route and products yielded but also the demand variability and setting the market price which can further affect the profitability and feasibility of the biomass supply chain (Lin et al., 2013). The demand variability of the biomass-derived products is often impacted by several factors (e.g. quality of biomass, price of the products, availability of the raw material, competitive market, etc.). For example, investing in biogas production industry would be a very risky act in Malaysia, as the nation's liquefied natural gas (LNG) had dominated the gas market (Malaysia is the fifth largest exporter of LNG in the world in 2019) (Energy Information Administration (EIA), 2021). In fact, the low market demand in Malaysia results in the hindrance of the development of the biogas-related industry. Therefore, to meet the challenge of demand variability, stochastic biomass supply chain models will be needed to forecast and predict demand response.

The instability of biomass-derived product price is attributed to the demand and quality of the products. At a regional level, the fluctuating prices of products have been disproportionate with the product fluctuations, causing the pricing of the yielded products to become inconsistent. Khatiwada et al. (2016) stated that the fluctuation of biomass-derived electricity price would eventually impact the feasibility of the overall biomass supply chain substantially. Typically, the unit costs for raw material and the biomass-derived products are expressed as fixed variables in techno-economic analysis which, therefore cause the results to be unrealistic and less reliable. It has been indicated that the feasibility of the biomass supply chain strongly depends on the biomass market where its inconsistency will eventually lead to a high level of risk management. As such, the sensitive correlation between price and other manipulative variables needs to be paid attention as they pose a great impact on developing a feasible biomass supply chain.

Beyond technological challenges and their uncertainties in the supply chain, policy selection could also, be one of the decisive criteria to be included in the stochastic biomass supply chain. The induction of nation's relevant regulations and policies (i.e., feed-in tariff system (FIT) from Renewable Energy Act, Renewable Energy Policy and Action Plan, Green Technology Financing Scheme (GTFS), etc. (International Energy Agency (IEA), 2019)), would cause the biomass industries to face potential compliance issues and operating cost increment (How et al., 2019). The failure of finding common ground for cooperation on policy-related matters between government and industries may lead to serious consequences such as potential social scandal, higher costing, or project delay (Yatim et al., 2016). Given that the policy selection will continue to play important role in the biomass industries to drive the development of renewable energy in Malaysia, the strategic model formulation that considers policy selection decisions for the sustainable biomass supply chain is highlighted in this chapter later.

The aforementioned research works had shown how biomass availability, biomass quality, and fluctuating price can significantly affect the feasibility of the supply chain. This reveals the necessity of incorporating these uncertainties into the stochastic biomass supply chain model. This chapter aims to provide an overview of the key uncertainties to be considered in the stochastic biomass supply chain model, then followed by three case studies that deal with (i) biomass selection decision, (ii) facility location decision, and (iii) policy selection decision, to demonstrate the application of the developed stochastic model.

2 Biomass Selection Decision

The Monte Carlo model can be utilized to perform decision-making such as the selection of biomass for the conversion process. Apart from biomass or product pricing, biomass quality is also one of the criteria that will affect the feasibility of the conversion process. Few researchers have considered numerous biomass qualities (e.g., moisture content (Ngan et al., 2020); moisture and ash content (Aboytes-Ojeda et al., 2019)) in their developed model. This section demonstrates the usage of the Monte Carlo model to select the optimal type of palm-based biomass (i.e., palm kernel shell (PKS), empty fruit bunches (EFB), and mesocarp fiber (MF)) for biomass gasification process with the consideration of their respective biomass qualities. The methodology to perform decision-making for biomass selection involves six general steps as follows:

(i) Data collection and pre-processing
(ii) Process simulation and validation of biomass conversion process
(iii) Generation of design matrix from Design of Experiment (DoE) software
(iv) Perform simulation based on the design matrix extracted from DoE software
(v) Extraction of the generic correlation equation
(vi) Formulation of Monte Carlo model

Note that the explanations of each step is presented in Sect. 2.1 (step (ii) to step (v)) and Sect. 2.2 (step (vi)).

2.1 Formulation of Generic Correlation Equation

The integrated use of a *process simulation* software and *Design of Experiment (DoE)* software is to formulate the generic correlation equation to be integrated into the Monte Carlo evaluation model. Firstly, the biomass conversion process can be simulated or modified *via* process simulation software. In this work, Aspen Plus and Design Expert software are used. Before simulating the desired process in Aspen Plus, a few information is required:

(i) Process flowsheet diagram
(ii) Process stream information (i.e., temperature, pressure, and other relevant information)
(iii) Operating conditions of the equipment.

For this case, the process flowsheet diagram and other required information are adapted from Han et al. (2017) whereby the authors simulated a downdraft biomass gasification process. The simulated flowsheet is illustrated in Fig. 2, whereas the significant operating conditions used are tabulated in Table 1. Before proceeding into the simulation environment, setting up of the simulation environment is significant. Two conventional components were input into the components that are biomass and ash. The enthalpy and density model selected for the two aforementioned conventional components are HCOALGEN and DCOALIGT. On top of that, due to the combination of non-conventional and conventional components in the process stream, the stream class MCINCPSD were defined. After defining the required physical property method, the simulation model can be developed based on the process flowsheet. The flowsheet is distributed into three sections (i.e., pre-treatment, gasification, and syngas clean up). The pre-treatment of biomass begins with the mixing of 80 kg of ambient wet biomass with ambient air (comprise of 78% nitrogen and 21% oxygen). The air to fuel ratio is 1.38, the amount of ambient air to be mixed with the wet biomass is 110.4 kg. Subsequently, the mixture of ambient air and wet biomass is transferred into the drier to undergo drying process to decrease the biomass moisture content to 8.91 wt%. The drier selected in Aspen Plus is **RStoic** block. The reduction of biomass moisture content is performed using FORTRAN calculator to be able to reduce varying moisture content of biomass into the system to 8.91 wt%. Subsequently, the moist air will be separated from the biomass *via* liquid–gas separation process in the moist air separator (default ID as **Flash2** in Aspen Plus environment). The dry biomass will then be transferred to the decomposer that is the **RYield** reactor to be broken down into its conventional elemental state (i.e., carbon, hydrogen, nitrogen, sulfur, oxygen, ash, volatile matter, and fixed carbon) using another FORTRAN calculator. It is worthy to note that the energy consumed by the gasifier is provided by the heat released during decomposition process. This is achieved by using the energy stream, QDECOMP, to link the decomposer to the gasifier. After undergoing decomposition process, the dry biomass stream that has been broken down into their conventional elemental state will enter a separator (default ID **Sep2** in Aspen Plus environment). The separator is used to separate a portion of the carbon to be treated as the unreacted char, whereby the split fraction used is 0.1. The solid dry biomass stream exiting the separator will be mixed with heated air (comprised of 78% nitrogen and 21% oxygen) of temperature 150 °C using Mixer_2 before transferred to the gasifier to undergo gasification process. The gasifier reactor's default ID in Aspen Plus simulation is **RGibbs** reactor. The downdraft biomass gasification process can be split into three zones (i.e., pyrolysis, oxidation, and reduction) as shown in Table 2. Different reactions will occur at different zones. The first zone, pyrolysis zone, dried biomass is pyrolyze into volatiles and char. Several processes occur in the next zone, oxidation zone (i.e., hydrogen oxidation, carbon monoxide oxidation, light hydrocarbon oxidation, heavy hydrocarbon oxidation, and char partial oxidation). Last zone, reduction zone will have the water gas shift reaction, Boudouard reaction, water gas reaction, methanation, and steam methane reforming. The reactions occurring at the reduction zone were input as restricting chemical reactions. At the same time, the previously separated portion of unreacted char will be heated to the same temperature (856.17 °C) as GASOUT stream from the gasifier to mix the two streams using Mixer_3. The outlet gas stream from Mixer_3, MGAS, is the final gas product stream of the gasification process with unreacted char being a minor constituent in the stream. The last stage will be the syngas clean-up. The stream MGAS leaving Mixer_3 will move into the cyclone (default ID in Aspen Plus environment is **SSplit**) to remove the unreacted char. The main product stream leaving the cyclone is HSYNGAS (syngas containing water). The syngas stream will be cooled to ambient temperature using a cooler before heading into Separator_2 (default ID is **Sep2** in Aspen Plus). The function of Separator_2 is to remove the water content from the clean syngas stream.

Validation of the simulated process with literature sources is required to ensure the accuracy of the simulated process. Subsequently, the design matrix can be extracted from DoE software. The design matrix represents the required number of simulation runs to be fulfilled in order to extract the formulated generic correlation equation. The selection of design mode is the first step in the DoE software to extract the design matrix. There are several available design modes within the DoE software, i.e., (i) factorial design mode, (ii) response surface design mode, (iii) mixture design mode, and (iv) custom design mode.

In this case, a full factorial design mode has been adopted (Teng et al., 2019). Six factorial was selected based on the number of input biomass quality variables. The biomass quality variables selected for input in the design matrix are (i) moisture content, (ii) ash content, (iii) carbon content, (iv) hydrogen content, (v) oxygen content, and (vi) sulfur content.

The DoE software will then require an input of the maximum and minimum value for each biomass quality. Subsequently, the response or result intended will be required to be defined in the model. In this case, the specific syngas yield, $S^{BIOMASS}$ (kg syngas/kg biomass) was defined as the desired response. Once the required input

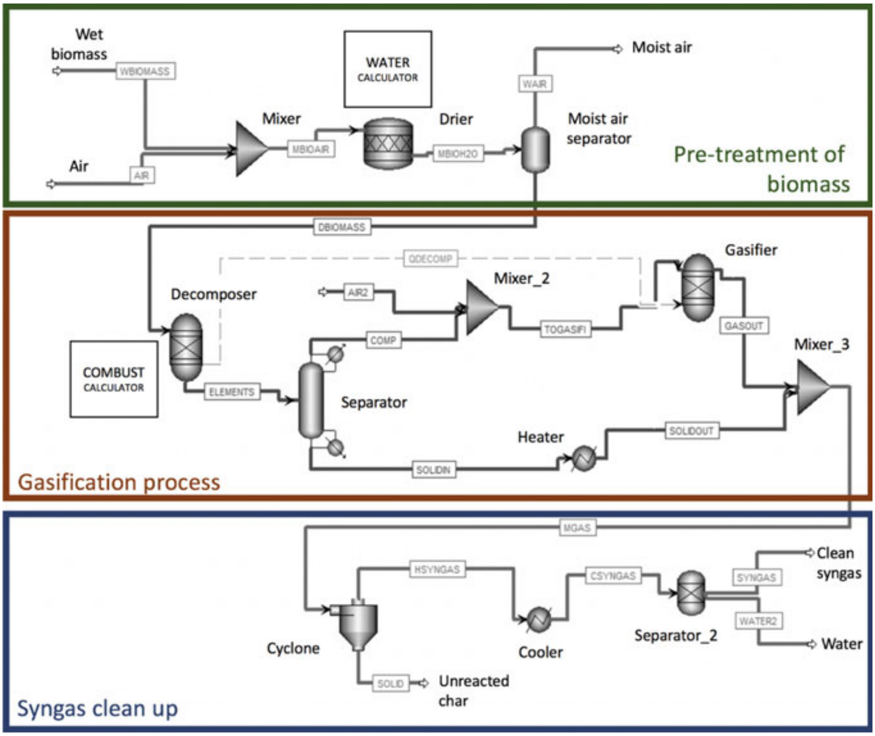

Fig. 2 Process simulation of biomass gasification process

Table 1 Fixed parameters used for this case study (Han et al., 2017)

Parameter	Unit	Value
Split fraction for unreacted carbon	–	0.1
Air inlet to gasifier	kg/hr	110
Air to fuel ratio	kg/kg	1.38
Temperature of inlet air	°C	150
Wet biomass into the system	kg/hr	80
Moisture content after drying	wt%	8.91
Outlet temperature of gasifier	°C	856.17

has been entered, the design matrix is then generated by the software. It is worthy to note that all the simulated runs of the design matrix require manual screening to ensure they meet the constraints shown in Eqs. (1) and (2). Both constraint equations require ensuring the summation of both proximate analysis and ultimate analysis to be at 100%, once the design matrix has been fulfilled, the generic correlation equation relating biomass quality to specific syngas yield can be extracted.

Table 2 Biomass gasification process reactions (adopted from Han et al., 2017)

Reaction name	Reaction equation	Reaction zone
Pyrolysis	Dried biomass $\rightarrow$ volatiles + char	Pyrolysis
H_2 oxidation	$H_2 + 0.5O_2 \rightarrow H_2O$	Oxidation
CO oxidation	$CO + 0.5O_2 \rightarrow CO_2$	Oxidation
Light hydrocarbon oxidation	$C_{1.16}H_4 + 1.58O_2 \rightarrow 1.16CO + 2H_2O$	Oxidation
Heavy hydrocarbon oxidation	$C_6H_{6.2}O_{1.2} + 4.45O_2 \rightarrow 6CO + 3.1H_2O$	Oxidation
Char partial oxidation	$C + 0.5O_2 \rightarrow CO$	Oxidation
Water gas shift	$CO + H_2O \leftrightarrow CO_2 + H_2$	Reduction
Boudouard	$C + CO_2 \leftrightarrow 2CO$	Reduction
Water gas	$C + H_2O \leftrightarrow CO + H_2$	Reduction
Methanation	$C + 2H_2 \leftrightarrow CH_4$	Reduction
Steam methane reforming	$CH_4 + H_2O \leftrightarrow CO + 3H_2$	Reduction
H_2S formation	$H_2 + S \rightarrow H_2S$	–
NH_3 formation	$0.5N_2 + 1.5H_2 \leftrightarrow NH_3$	–

$$Q^{\mathrm{FC}} + Q^{\mathrm{VM}} + Q^{A} + Q^{\mathrm{MC}}\ \mathrm{wt\%} \tag{1}$$

$$Q^{H} + Q^{C} + Q^{O} + Q^{S} + \mathrm{Q}^{\mathrm{N}} = 100\mathrm{wt\%} \tag{2}$$

Q^{FC}, Q^{VM}, Q^{A}, and Q^{MC} denote the weight composition of fixed carbon, volatile matter, ash, and moisture content of the biomass; whileQ^{H}, Q^{C}, Q^{O}, Q^{S} and Q^{N} denote the weight composition of hydrogen, carbon, oxygen, sulfur, and nitrogen of the biomass.

2.2 *Monte Carlo Model Formulation for Biomass Selection*

Net present value (NPV) (expressed in Eq. (3)) is used as an indicator to compare the feasibility of utilization of each type of biomass in consideration, where NCF_t refers to the net cash flow in year t, while in refers to the discount rate.

$$\mathrm{NPV} = \sum\nolimits_{t} \frac{\mathrm{NCF}_t}{(1 + in)^t} \tag{3}$$

Equation (4) is used to determine NCF_t, where the input and output cash flows are denoted as $\mathrm{CF}_t^{\mathrm{IN}}$ and $\mathrm{CF}_t^{\mathrm{OUT}}$ respectively.

$$\mathrm{NCF}_t = (\mathrm{CF}_t^{\mathrm{IN}} - \mathrm{CF}_t^{\mathrm{OUT}}) \tag{4}$$

The input cash flows, $\mathrm{CF}_t^{\mathrm{IN}}$ depicts the revenue obtained from the sales of value-added products from the biomass conversion process. In this case, it would be the sales of syngas produced from the biomass gasification process. $\mathrm{CF}_t^{\mathrm{IN}}$ can then be obtained from the multiplication of three variables, specific syngas yield, S^{BIOMASS}, the amount of biomass required, $\mathrm{Biomass}_t^{\mathrm{IN}}$ and the selling price of syngas, C_t^{SYNGAS}.

$$\mathrm{CF}_t^{\mathrm{IN}} = S^{\mathrm{BIOMASS}} \times \mathrm{Biomass}_t^{\mathrm{IN}} \times C_t^{\mathrm{SYNGAS}} \tag{5}$$

$\mathrm{CF}_t^{\mathrm{OUT}}$, on the other hand, is contributed by the capital expenditure (CAPEX) and operating expenditure (OPEX) (C^{CAPEX} and C_t^{OPEX}, respectively); and procurement cost for biomass (C_t^{PROCURE}) and coal (C_t^{PROCURE}) as shown in Eq. (6).

$$\mathrm{CF}_t^{\mathrm{OUT}} = C^{\mathrm{CAPEX}} + C_t^{\mathrm{OPEX}} + C_t^{\mathrm{PROCURE}} \tag{6}$$

On the other hand, C_t^{PROCURE} can be determined by multiplying the amount of the material to their respective unit cost, where C_t^{BIOMASS} and C_t^{COAL} refers to the acquisition cost of biomass and coal, respectively:

$$C_t^{\mathrm{PROCURE}} = (\mathrm{Biomass}_t^{IN} \times C_t^{\mathrm{BIOMASS}}) + (F_t^{\mathrm{COAL}} \times C_t^{\mathrm{COAL}}) \tag{7}$$

F_t^{COAL} can be calculated using Eqs. (8) and (9) whereby $\mathrm{Q}^{\mathrm{coal}}$ denotes the energy required to reduce the moisture content, $\mathrm{MC}_t^{\mathrm{IN}}$ and $\mathrm{MC}_t^{\mathrm{OUT}}$ represents the initial and final moisture content of biomass, respectively. On the other hand, T_{Final} and T_{Initial} denotes the final and initial temperature of the biomass, respectively. c denotes the specific heat capacity of water and $\mathrm{HV}^{\mathrm{coal}}$ denotes the heating value of coal.

$$\mathrm{Q}^{\mathrm{coal}} = \left(\mathrm{MC}_t^{\mathrm{IN}} - \mathrm{MC}^{\mathrm{OUT}}\right) \times \mathrm{Biomass}_t^{\mathrm{IN}} \times \mathrm{c} \times (T_{\mathrm{Final}} - T_{\mathrm{Initial}}) \tag{8}$$

$$F_t^{\mathrm{COAL}} = \frac{\mathrm{Q}^{\mathrm{coal}}}{\mathrm{HV}^{\mathrm{coal}}} \tag{9}$$

There is also a noteworthy constraint shown in Eq. (10) whereby the $\mathrm{Biomass}_t^{\mathrm{IN}}$ must be less than or equal to the $\mathrm{Biomass}_t^{\mathrm{SUPPLY}}$. If $\mathrm{Biomass}_t^{\mathrm{IN}}$ is greater than $\mathrm{Biomass}_t^{\mathrm{SUPPLY}}$, an alternative solution will have to be considered to ensure the demand is met.

$$\mathrm{Biomass}_t^{\mathrm{IN}} \leq \mathrm{Biomass}_t^{\mathrm{SUPPLY}} \tag{10}$$

Subsequently, a total of 10,000 randomized NPV samples are generated *via* the *Monte Carlo* simulation, where the values of $\mathrm{Biomass}_{\mathrm{EFB}}^{\mathrm{QUALITY}}$, $\mathrm{Biomass}_{\mathrm{PKS}}^{\mathrm{QUALITY}}$, $\mathrm{Biomass}_{\mathrm{MF}}^{\mathrm{QUALITY}}$, $\mathrm{Biomass}_t^{\mathrm{SUPPLY}}$, C_t^{BIOMASS} and C_t^{SYNGAS} for each sample is randomized based on the historical statistical data collected. With this, the supply uncertainty, biomass quality uncertainty, price variation of biomass, and syngas can be incorporated into the model. The NPV and payback period (PBP) are the expected outcome from the model whereby the PBP can be determined through the subtraction method.

2.3 Illustrative Example

A palm-based biomass gasification plant is used as an illustrative case study to demonstrate the utilization of the Monte Carlo model to perform decision-making for biomass selection. The palm-based biomasses considered are EFB, PKS, and MF. The randomized parameters considered in this case study include syngas price, biomass supply, cost of biomass, and biomass quality whereby their respective value is tabulated in Table 3.

The mean, μ, and standard deviation, σ are obtained from the calculation of the minimum and maximum values for each of the uncertainty. The minimum and maximum values can be extracted from the historical statistical data for the uncertainties. On the other hand, other non-randomized parameters that were used in developing the case study model are shown in Table 4. It is worthy to note that the current case study does not consider the transportation cost for the materials (i.e., biomass and syngas).

The validation of the simulated process flowsheet (Fig. 2) has been tabulated in Table 5. The process is simulated, modified, and validated based on the works of Han et al. (2017). It is observable that the percentage difference calculated is relatively low with the highest being nitrogen content with a 5.80% difference. This is partially due to the under-production of one of the components that is methane in the equilibrium modeling environment (Song et al., 2013).

After validation of the simulated process, the next step was to extract the design matrix from DoE software and perform the simulation based on the design matrix. Subsequently, the generic correlation equation relating biomass quality to specific syngas yield was extracted (see Eq. (11)). The equation extracted met with a few criteria that ensure the applicability of the equation. One of the criteria is the equation's Prob > F value for lack of fit was 0.3668 that implies the equation provides high probability for good fitting. On top of that, the equation has an R^2 value of 0.9020 whereas the adjusted R^2 value, and the predicted R^2 value are 0.8917, and 0.8686, respectively. If the predicted R^2 value and adjusted R^2 value have a difference smaller than 0.20, it signifies that the equation is used which is the case reflected here (StatEase, 2020).

$$\begin{aligned}\text{specific syngas yield} = {} & 2.09922 + 1.80801 \times 10^{-3}\left(Q^{\mathrm{MC}}\right) \\ & - 5.26,803 \times 10^{-3}\left(Q^{A}\right) + 9.59237 \times 10^{-3}\left(Q^{C}\right) \\ & - 0.033116\left(Q^{H}\right) - 4.39309 \times 10^{-3}\left(Q^{O}\right) \\ & - 4.31267 \times 10^{-3}(Q^{S}) \end{aligned} \tag{11}$$

Table 3 Randomised parameters used for this case study

Parameter	Remark	Value	Reference
$\text{Biomass}_t^{\text{SUPPLY}}$ (kg/hour)	EFB PKS MF	$\mu = 82{,}206.75$; $\sigma = 3675.36$ $\mu = 26{,}156.69$; $\sigma = 1169.43$ $\mu = 48{,}576.72$; $\sigma = 2171.81$	DQS Certification (2018)
$\text{Biomass}_{\text{EFB}}^{\text{QUALITY}}$ (wt %)	Moisture content Ash content Carbon content Hydrogen content Oxygen content Sulfur content	$\mu = 7.79$; $\sigma = 2.60$ $\mu = 6.75$; $\sigma = 1.14$ $\mu = 42.28$; $\sigma = 9.23$ $\mu = 6.70$; $\sigma = 1.37$ $\mu = 42.88$; $\sigma = 8.74$ $\mu = 0.31$; $\sigma = 0.15$	Sohni et al., (2018) Mahlia et al., (2001) Yoo et al., (2019)
$\text{Biomass}_{\text{PKS}}^{\text{QUALITY}}$ (wt %)	Moisture content Ash content Carbon content Hydrogen content Oxygen content Sulfur content	$\mu = 5.87$; $\sigma = 4.03$ $\mu = 7.48$; $\sigma = 6.05$ $\mu = 47.8$; $\sigma = 6.51$ $\mu = 7.66$; $\sigma = 1.92$ $\mu = 40.22$; $\sigma = 4.12$ $\mu = 0.7$; $\sigma = 0.71$	Sohni et al., (2018) Mahlia et al., (2001) Ahmad et al., (2014) Aziz et al., (2011)
$\text{Biomass}_{\text{MF}}^{\text{QUALITY}}$ (wt %)	Moisture content Ash content Carbon content Hydrogen content Oxygen content Sulfur content	$\mu = 5.06$; $\sigma = 0.43$ $\mu = 4.9$; $\sigma = 4.95$ $\mu = 46.29$; $\sigma = 1.29$ $\mu = 8.30$; $\sigma = 3.25$ $\mu = 39.37$; $\sigma = 3.78$ $\mu = 0.49$; $\sigma = 0.26$	Mahlia et al., (2001) Aziz et al., (2011) Garba et al., (2017)
C_t^{BIOMASS} (USD/t)	EFB PKS MF	$\mu = 120$; $\sigma = 33.6$ $\mu = 60$; $\sigma = 31.2$ $\mu = 6$; $\sigma = 5.04$	Abas et al. (2011) Lam et al., (2013) Reduan (2017) Lo et al., (2021) Agensi Inovasi Malaysia (2013)
C_t^{SYNGAS} (USD/t)		$\mu = 470.4$; $\sigma = 100.8$	Zuldian et al., (2017)

Following the formulation of the generic correlation equation, the next step would be to evaluate the economic performance *via* Monte Carlo simulation. Figure 3 illustrates the probability density result for the NPV value. It can be observed that MF has a greater probability to achieve a higher NPV value that is 16% to achieve a probability of approximately USD 24 million. On the other hand, PKS has a lower NPV achievable that is approximately 16.5% to achieve an NPV of approximately USD 22 million. EFB then poses the least favorable NPV outcome among the three types of palm-based biomass with a 17% of achieving an NPV value of approximately USD 18 million. Three factors contributed to the resulting outcome, i.e., (i) cost of purchasing biomass, (ii) carbon content of biomass, and (iii) standard deviation of uncertainties.

Table 4 Fixed parameters used for this case study

Parameter	Remark	Value	Reference
MC^{OUT}(wt %)	Desired quality	4	–
in(%)	Common assumption	10	–
t	Expected minimum lifespan	20	–
C^{CAPEX}(M USD)	–	5.3	Susanto et al. (2018) Aghabararnejad et al. (2015)
C_t^{OPEX}(M USD)	–	0.38	AlNouss et al. (2020) Spath et al. (2005)

Table 5 Validation of simulated process flowsheet

Syngas composition	Units	Simulated results	Reference results	Percentage difference (%)
CO	mol%	20.98	20.93	0.24
H_2	mol%	18.07	18.32	1.36
CO_2	mol%	13.55	12.87	5.28
N_2	mol%	47.39	44.79	5.80

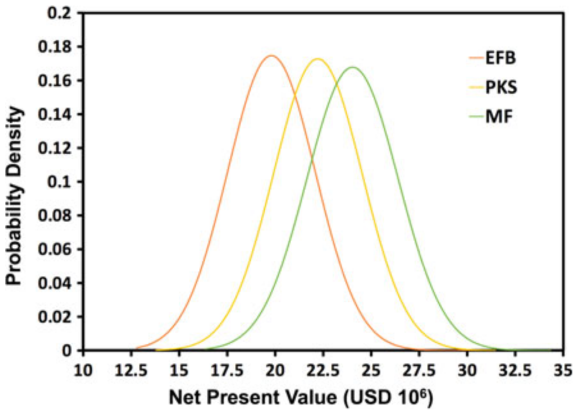

Fig. 3 Probability Density of NPV for biomass gasification plant

Firstly, it is observable from Table 3 that the mean acquisition price of MF is the lowest among the three types of palm-based biomass. Not to mention there is a significant difference between MF and EFB of approximately 95%. Thus, this will ultimately affect the total procurement cost, $C_t^{PROCURE}$ (see Eq. (11)). A lower

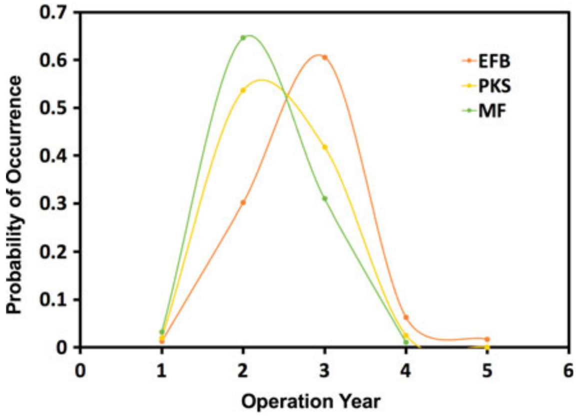

Fig. 4 Probability occurrence of PBP for biomass gasification plant

biomass acquisition cost will result in a lower procurement cost and operating cost that will ultimately increase the profit gained by the process. Secondly, the carbon content of biomass would also affect the syngas produce from the biomass gasification process. This is because there are two products formed during the biomass gasification process containing the carbon element that is carbon monoxide and carbon dioxide. On top of that, carbon monoxide is the critical component of syngas. Therefore, a higher amount of carbon content would be favorable. Table 3 shows that EFB offers the lowest average carbon content. Apart from that, it is noticeable that the standard deviation of the uncertainties for EFB is relatively greater in value as compared to MF and PKS. This is resulting from a larger difference in the minimum and maximum value extracted from the historical statistical data of the uncertainties. For instance, the mean and standard deviation of carbon content for EFB are 42.28 wt% and 9.23 wt%, respectively, whereas the mean and standard deviation of carbon content for PKS are 47.8 wt% and 6.51 wt%, respectively. On the other hand, Fig. 4 shows the payback period of the gasification process for the three types of palm-based biomass. In agreement with the obtained NPV results, MF has a higher probability to offset the capital cost expenditure earlier as compared to EFB and PKS. Specifically, MF has a probability of 68% to offset the capital cost expenditure in the second year of plant operation. Hence, the selected biomass that will be more feasible is MF.

3 Facilities Location Decision

Apart from the aforementioned biomass selection, Monte Carlo simulation can also be utilized in location selection for biomass conversion plants. Previously in Sect. 2, the biomass that showed a more favorable outcome was MF. Therefore, this section will target biomass conversion process using specifically MF as the feedstock. As the influence of biomass quality has been considered in the previous case study, biomass quality uncertainty will not be incorporated into the model developed in this section. This section will highlight more on location selection. Different locations pose different effects on the total transportation cost due to several variables (i.e., number of trips, distance, etc.). Hence, this section will demonstrate the use of Monte Carlo to select a financially feasible location for an MF-based gasification plant.

3.1 Model Formulation for Location Selection

Similar to the former case study, NPV and PBP are used to evaluate the economic feasibility of the candidate locations for setting up the biomass conversion plant. The same formulations (Eqs. (3) and (4)) are used to compute the overall NPV for this case study, while PBP is determined using the same aforementioned subtraction method.

Note that in this case study, $\mathrm{CF}_t^{\mathrm{IN}}$ and $\mathrm{CF}_t^{\mathrm{OUT}}$ are determined using the Eqs. (12) and (13), respectively.

$$\mathrm{CF}_t^{\mathrm{IN}} = F_t^{\mathrm{SYNGAS}} \times C_t^{\mathrm{SYNGAS}} \tag{12}$$

$$\mathrm{CF}_t^{\mathrm{OUT}} = C^{\mathrm{CAPEX}} + C_t^{\mathrm{OPEX}} + C_t^{\mathrm{PROCURE}} + C_t^{TR} \tag{13}$$

where F_t^{SYNGAS} refers to the amount of syngas produced, while C_t^{TR} denotes the total transportation cost.

The procurement cost of raw material, C_t^{PROCURE} is determined using Eq. (7), whereas C_t^{TR} is calculated using Eq. (14), where d^S refers to the traveling distance between biomass supply and the MF-based gasification plant; d^D refers to the traveling distance between the MF-based gasification plant and the demand point (port); $\mathrm{Cap}^{\mathrm{TRUCK}}$ denotes the vehicle load limit; while the fuel consumption rate of the vehicle and the respective fuel price in year t is expressed as ψ^{FUEL} and C_t^{FUEL}, respectively. For a round trip, the distances traveled have to be multiplied by "2" as shown in Eq. (14).

$$C_t^{\mathrm{TR}} = 2 \times \frac{\left(\mathrm{Biomass}_t^{\mathrm{IN}} \times d^S + F_t^{\mathrm{SYNGAS}} \times d^D\right)}{\mathrm{Cap}^{\mathrm{TRUCK}}} \times \psi^{\mathrm{FUEL}} \times C_t^{\mathrm{FUEL}} \tag{14}$$

Thereafter, *Monte Carlo* simulation (10,000 samples) is conducted to determine the probability profile for NPV and PBP for each location with the consideration of the uncertainties for five input parameters (i.e., F_t^{SYNGAS}, $\mathrm{Biomass}_t^{\mathrm{SUPPLY}}$, C_t^{BIOMASS}, C_t^{FUEL} and C_t^{SYNGAS}). Then, the optimal location to set up the MF-based gasification plant.

3.2 Illustrative Example

In this illustrative example, the developed model was used to select the optimal location to set up an MF-based gasification plant. Three candidate locations (Plant A, Plant B, and Plant C) have been considered in this case study. The distance between each location and specifications (i.e., loading capacity and fuel consumption) for the transportation vehicle are the significant data required to be collected. The respective distance data is tabulated in Table 6. Additionally, two types of transportation modes, i.e., a dump truck (truck A) for MF delivery and a fuel tanker (Truck B) for syngas delivery, are considered in this example (note: the specifications of the transportation modes are tabulated in Table 7).

On the other hand, the randomized input parameters for the developed *Monte Carlo model* are listed in Table 8, whereas Table 9 shows the fixed parameters used in the developed model. Note that the mean, μ, and standard deviation, σ shown in Table 8 are obtained from the historical statistical data.

Figure 5 showed the NPV results for the three plant locations investigated. Based on Fig. 5a, it shows that the plant locations seem to have minimal impact on the NPV result. It is worthy to note that the amount of biomass required to meet the demand is less than the biomass availability. However, it is assumed that all the biomass will be transported to the gasification plant, while the excessive biomass will be stored for future usage. As the biomass feed is excess, the number of trips taken to complete the transfer of biomass to the MF-based gasification plant will be more than the number of trips taken to transfer syngas from the plant to the port. Another noteworthy statement is that all mean and standard deviation of the uncertainty listed in Table 8 are the same for all three plant locations. The only variation would be the total transportation cost that is influenced by distance and number of trips. With a zoom-in view (Fig. 5b), it is found that Plant C has a slightly higher probability (approximately 0.1%) than that of the other two plants in obtaining an NPV value of USD 41.5 million. As a result, Plant C poses the lowest mean and standard deviation among the three plants (USD 41.58 million ± 4.94 million). Despite having the lowest mean, the lowest standard deviation implies that there would be less risk

Table 6 Fixed parameters used for this case study (Lo et al., 2020)

Plant	d^S(km)	d^D(km)
Plant A	18.6	78.5
Plant B	42.8	41
Plant C	80.4	24.2

Table 7 Specification for transportation modes

Truck	Truck type	Loading capacity (t)	Fuel consumption (l/100 km)
Truck A	Dump truck	30	47
Truck B	Fuel tanker	30	43

Table 8 Randomized parameters used for this case study

Parameter	Value	Reference
$\text{Biomass}_t^{\text{SUPPLY}}$(t/year)	$\mu = 48{,}576.72; \sigma = 2171.81$	DQS Certification (2018)
C_t^{BIOMASS} (USD/t)	$\mu = 6; \sigma = 5.04$	Lo et al. (2021) Agensi Inovasi Malaysia (2013)
C_t^{SYNGAS} (USD/t)	$\mu = 470.4; \sigma = 100.8$	Zuldian et al. (2017)
C_t^{FUEL} (USD/L)	$\mu = 0.44; \sigma = 0.21$	Trading Economics (2020)
F_t^{SYNGAS} (MWth)	$\mu = 3262.09; \sigma = 1140.58$	MarketsandMarkets Research Private Ltd. (2020)

Table 9 Fixed parameters used for this case study

Parameter	Value	Reference
in(%)	10	–
t	20	–
C^{CAPEX}(M USD)	5.3	Susanto et al. (2018) Aghabararnejad et al. (2015)
C_t^{OPEX}(M USD)	0.38	AlNouss et al. (2020) Spath et al. (2005)

of fluctuation of the NPV for Plant C. To note, the lower mean observed in Plant C is partially due to the greater distance between the biomass source and Plant C that is d^S. As previously mentioned, the biomass will be in excess, thus, requiring more trips taken to transport the biomass to the gasification plant. Additionally, the fuel consumption of the dump truck is greater than the fuel consumption of the fuel tanker (see Table 7). The combinatory effect of a greater d^S, a greater number of trips and a higher fuel consumption rate for the dump truck directly increase total transportation cost. On the other hand, the mean and standard deviation for NPV for Plant A and Plant B is USD 41.66 million $\pm$ 4.98 million and USD 41.65 million $\pm$ 4.99 million, respectively. Looking at the probability of occurrence for PBP in Fig. 6, it is observable that Plant B has a higher probability to offset the capital cost invested when it reaches 1.75 years of operations. However, looking into Fig. 6(b), it is observable that Plant A has a higher probability of approximately 0.4% to offset the capital investment earlier than is into 1 year of operation. Hence, after careful consideration of the results obtained, Plant A is selected as the more feasible plant location.

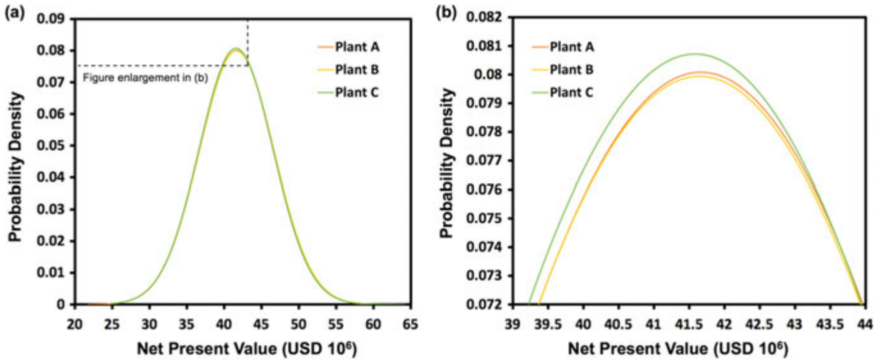

Fig. 5 **a** NPV for Plant A, Plant B and Plant C, **b** enlargement of a section of (**a**)

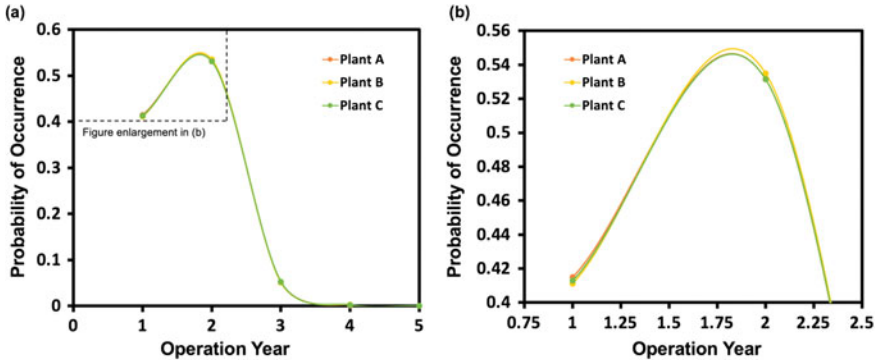

Fig. 6 **a** PBP for Plant A, Plant B and Plant C, **b** enlargement of a section of (**a**)

4 Policy Selection Decisions

Aside from the aforementioned process pathway selection, the utility of *Monte Carlo* simulation can be extended to policy selection. To date, it has been used as a supporting tool to help decision-maker in determining the optimal policy for various problems, including but not limited to pricing policy for parking management (Wang et al., 2021); E-hailing platform policy (Shou et al., 2020); replacement policy for equipment composed multiple non-identical components (Barde et al., 2019); and renewable energy schemes (Chou & Ongkowijoyo, 2014). This section, on the other hand, demonstrates its utility in selecting a policy (or action plan) to mitigate the overall business risk of a biomass-based polygeneration system.

4.1 Model for Biomass-Based Polygeneration System

Again, both NPV and PBP are used to evaluate the effectiveness of the available action plans. Note that since the monthly variations of the parameters are considered in this case study, the formulations used to determine NPV have now been revised to incorporate index m (for month). For instance, NPV is now determined using Eq. (15), where $\mathrm{NCF}_{m,t}$ refers to the net cash flow at month m in year t.

$$\mathrm{NPV} = \sum_{t} \sum_{m} \frac{NCF_{m,t}}{(1 + in)^t} \tag{15}$$

Equation (16) is used to determine $\mathrm{NCF}_{m,t}$, where the input and output cash flows are denoted as $\mathrm{CF}^{\mathrm{IN}}_{m,t}$ and $\mathrm{CF}^{\mathrm{OUT}}_{m,t}$ respectively, TAX refers to the corporate tax rate, while ITA indicates the tax exemption indicator. It is worth noting that the qualifying rate and limit for the exemption are set at 80% and 85%, respectively (Lembaga Hasil Dalam Negeri Malaysia (LHDN), 2018).

$$\mathrm{NCF}_{m,t} = \left(\mathrm{CF}^{\mathrm{IN}}_{m,t} - \mathrm{CF}^{\mathrm{OUT}}_{m,t}\right) \times (1 - \mathrm{TAX}) + \mathrm{ITA} \times \mathrm{TAX} \forall t \in T, \quad \forall m \in M \tag{16}$$

Generally, polygeneration plant yields multiple profitable products. Taking a polygeneration plant which consists of pyrolysis process and co-generation as an example, the $\mathrm{CF}^{\mathrm{IN}}_{m,t}$ can be determined using Eq. (17):

$$\mathrm{CF}^{\mathrm{IN}}_{m,t} = F^{\mathrm{OIL}}_{m,t} \times C^{OIL}_{m,t} + \mathrm{Elec}^{\mathrm{EXP}}_{m,t} \times C^{\mathrm{FIT}} \quad \forall t \in T, \forall m \in M \tag{17}$$

where the first term refers to the sales obtained from selling bio-oil ($F^{\mathrm{OIL}}_{m,t}$) with bio-oil price of $C^{\mathrm{OIL}}_{m,t}$; while the second term shows the profit obtained by exporting the generated power ($\mathrm{Elec}^{\mathrm{EXP}}_{m,t}$) with a feed-in-tariff (FiT) rate of C^{FIT}.

Equations (18) to (20) show the mass conversion equations for the three pyrolysis products, which include $F^{\mathrm{OIL}}_{m,t}$, syngas ($F^{\mathrm{GAS}}_{m,t}$) and biochar ($F^{\mathrm{CHAR}}_{m,t}$):

$$F^{\mathrm{OIL}}_{m,t} = \mathrm{Biomass}^{\mathrm{DRY}}_{m,t} \times y^{\mathrm{OIL}} \quad \forall t \in T, \forall m \in M \tag{18}$$

$$F^{\mathrm{GAS}}_{m,t} = \mathrm{Biomass}^{\mathrm{DRY}}_{m,t} \times y^{\mathrm{GAS}} \quad \forall t \in T, \forall m \in M \tag{19}$$

$$F^{\mathrm{CHAR}}_{m,t} = \mathrm{Biomass}^{\mathrm{DRY}}_{m,t} \times y^{\mathrm{CHAR}} \quad \forall t \in T, \forall m \in M \tag{20}$$

where $\mathrm{Biomass}^{\mathrm{DRY}}_{m,t}$ refers to the mass flow rate of dried biomass fed into the pyrolyser; while y^{OIL}, y^{GAS} and y^{CHAR} denote the product yield of bio-oil, syngas, and biochar, respectively.

It is worth noting that $F_{m,t}^{\mathrm{GAS}}$ contains various high energy content gases g (i.e., CO, H_2 and CH_4). Therefore, it can be used to produce energy (power ($\mathrm{Elec}_{m,t}^{\mathrm{GEN}}$) and heat ($\mathrm{Thermal}_{m,t}^{\mathrm{GEN}}$)) *via* co-generation unit (see Eqs. (21) and (22)). Based on commercial gas engine performance data, the amount of thermal energy recovered from a co-gen process is 1.2 times the amount of electricity being generated (GE, 2018).

$$\mathrm{Elec}_{m,t}^{\mathrm{GEN}} = \sum_{g}\left(F_{m,t}^{\mathrm{GAS}} \times y_{g}^{PY} \times \mathrm{LHV}_{g}\right) \times \xi^{\mathrm{COGEN}} \quad \forall t \in T,\ \forall m \in M \tag{21}$$

$$\mathrm{Thermal}_{m,t}^{\mathrm{GEN}} = 1.2 \times \mathrm{Elec}_{m,t}^{\mathrm{GEN}} \quad \forall t \in T,\ \forall m \in M \tag{22}$$

where y_{g}^{PY} and LHV_{g} refer to the molar composition and low heating value of gas g, respectively, while ξ^{COGEN} denotes the conversion efficiency of the co-generation unit.

$\mathrm{Elec}_{m,t}^{\mathrm{GEN}}$ can be used to fulfill the power demand for the pyrolyser ($\mathrm{Elec}_{m,t}^{\mathrm{REQ}}$; computed through Eq. (23)). If $Elec_{m,t}^{\mathrm{GEN}}$ is less than $\mathrm{Elec}_{m,t}^{\mathrm{REQ}}$, the balance will be covered by importing external power ($\mathrm{Elec}_{m,t}^{\mathrm{IMP}}$). In contrast, the excess power ($\mathrm{Elec}_{m,t}^{\mathrm{EXP}}$) will be exported back to the grid. This can be defined as Eq. (24), where ψ^{PY} refers to the thermal energy required to try per unit mass of biomass:

$$\mathrm{Elec}_{m,t}^{\mathrm{REQ}} = \mathrm{Biomass}_{m,t}^{\mathrm{DRY}} \times \psi^{\mathrm{PY}} \quad \forall t \in T,\ \forall m \in M \tag{23}$$

$$\mathrm{Elec}_{m,t}^{\mathrm{GEN}} + \mathrm{Elec}_{m,t}^{\mathrm{IMP}} = \mathrm{Elec}_{m,t}^{\mathrm{REQ}} + \mathrm{Elec}_{m,t}^{\mathrm{EXP}} \quad \forall t \in T,\ \forall m \in M \tag{24}$$

whereas $\mathrm{Thermal}_{m,t}^{\mathrm{GEN}}$ can be used to compensate for the thermal energy required during the biomass drying ($\mathrm{Thermal}_{m,t}^{\mathrm{REQ}}$; determined *via* Eq. (25)). Besides, the generated $F_{m,t}^{\mathrm{CHAR}}$ can also be used as a solid fuel to generate thermal energy. Coal ($F_{m,t}^{COAL}$) will be imported as additional solid fuel if the generated thermal energy from co-generation and char burning is insufficient to meet the energy consumption (see Eq. (26)):

$$\mathrm{Thermal}_{m,t}^{\mathrm{REQ}} = \mathrm{Biomass}_{m,t}^{\mathrm{IN}} \times \frac{\left(MC_{m,t}^{\mathrm{IN}} - MC^{\mathrm{OUT}}\right)}{100} \times \psi^{\mathrm{THERMAL}} \quad \forall t \in T,\ \forall m \in M \tag{25}$$

$$\begin{aligned}\mathrm{Thermal}_{m,t}^{\mathrm{REQ}} = {} & \left(F_{m,t}^{\mathrm{COAL}} \times \mathrm{LHV}^{\mathrm{COAL}} + F_{m,t}^{\mathrm{CHAR}} \times \mathrm{LHV}^{\mathrm{CHAR}}\right) \times \xi^{\mathrm{DRY}} \\ & + \mathrm{Thermal}_{m,t}^{\mathrm{GEN}} \quad \forall t \in T,\ \forall m \in M\end{aligned} \tag{26}$$

where $\mathrm{Biomass}_{m,t}^{\mathrm{IN}}$ refers to the amount of raw biomass sent to the polygeneration plant; $\mathrm{MC}_{m,t}^{\mathrm{IN}}$ and $\mathrm{MC}^{\mathrm{OUT}}$ present the moisture content before and after the drying process, respectively, the low heating values of coal and char are denoted as LHV^{COAL} and LHV^{CHAR}, respectively; $\psi^{THERMAL}$ indicate the thermal energy required to remove per mass unit of water content, while the drying efficiency is expressed as ξ^{DRY}.

$CF^{OUT}_{m,t}$, on the other hand, is contributed by the capital expenditure (CAPEX) and operating expenditure (OPEX) of unit u (C^{CAPEX}_{u} and $C^{OPEX}_{u,m,t}$ respectively); transportation cost ($C^{TR}_{m,t}$); procurement cost for imported electricity, biomass, and coal ($C^{PROCURE}_{m,t}$); and carbon penalty ($C^{PENALTY}_{m,t}$).

$$CF^{OUT}_{m,t} = \begin{cases} \left.\sum_{u} C^{CAPEX}_{u}\right|_{t=0} \\ \left.\sum_{u} C^{OPEX}_{u,m,t} + C^{TR}_{m,t} + C^{PROCURE}_{m,t} + C^{PENALTY}_{m,t}\right|_{t>0} \end{cases} \quad \forall t \in T,\ \forall m \in M \tag{27}$$

$C^{TR}_{m,t}$ considers the cost associated with the transportation of the materials (including biomass and bio-oil). To note, the conventional 10-t truck are used as the transportation mode in this section. It is expressed as follow:

$$C^{TR}_{m,t} = 2 \times \frac{\left(\text{Biomass}^{IN}_{m,t} \times d^{S} + F^{OIL}_{m,t} \times d^{D}\right)}{\text{Cap}^{TRUCK}} \times \psi^{FUEL} \times C^{FUEL}_{m,t} \quad \forall t \in T,\ \forall m \in M \tag{28}$$

where d^{S} refers to the traveling distance between biomass supply and the polygeneration plant; d^{D} refers to the traveling distance between the polygeneration plant and the demand point; Cap^{TRUCK} denotes the vehicle load limit; while the fuel consumption rate of the vehicle and the respective fuel price at month m in year t is expressed as ψ^{FUEL} and $C^{FUEL}_{m,t}$ respectively. For a round trip, the distance traveled has to be multiplied by "2" as shown in Eq. (28).

On the other hand, $C^{PROCURE}_{m,t}$ can be determined by multiplying the capacity of the imported material to their respective unit cost, where $C^{BIOMASS}_{m,t}$, $C^{COAL}_{m,t}$ and C^{ELEC} refer to the respective cost of biomass, coal, and imported electricity, respectively:

$$C^{PROCURE}_{m,t} = \text{Biomass}^{IN}_{m,t} \times C^{BIOMASS}_{m,t} + F^{COAL}_{m,t} \times C^{COAL}_{m,t} + \text{Elec}^{IMP}_{m,t} \times C^{ELEC} \quad \forall t \in T,\ \forall m \in M \tag{29}$$

In terms of $C^{PENALTY}_{m,t}$, it is expressed as the compensation cost required to recover the environmental damage caused by the carbon emission. It can be determined using Eq. (30):

$$C^{PENALTY}_{m,t} = C^{CO_2} \times \left(2 \times \frac{\left(\text{Biomass}^{IN}_{m,t} \times d^{S} + F^{OIL}_{m,t} \times d^{D}\right)}{\text{Cap}^{TRUCK}} \times \psi^{FUEL} \times y^{CO_2\_TR}\right.$$

$$+\mathrm{Elec}_{m,t}^{\mathrm{GEN}} \times y^{\mathrm{CO_2\_COGEN}} + F_{m,t}^{\mathrm{GAS}} \times y^{\mathrm{CO_2\_PY}}\Big) \quad \forall t \in T,\ \forall m \in M \tag{30}$$

where $y^{\mathrm{CO_2\_TR}}$, $y^{\mathrm{CO_2\_COGEN}}$, and $y^{\mathrm{CO_2\_PY}}$ refer to the estimated CO_2 emitted during transportation, co-generation unit, and pyrolysis process, while $C^{\mathrm{CO_2}}$ refers to the compensation cost required per unit of carbon emission.

The following two equations are applied to reflect the biomass availability constraint and bio-oil demand constraint, where $\mathrm{Biomass}_{m,t}^{\mathrm{AVAILABLE}}$ and $F_{m,t}^{OIL\_DEMAND}$ reflect the biomass availability and the bio-oil demand at month m in year t:

$$\mathrm{Biomass}_{m,t}^{\mathrm{AVAILABLE}} \geq \mathrm{Biomass}_{m,t}^{\mathrm{IN}} \quad \forall t \in T,\ \forall m \in M \tag{31}$$

$$F_{m,t}^{\mathrm{OIL}} \leq F_{m,t}^{\mathrm{OIL\_DEMAND}} \quad \forall t \in T,\ \forall m \in M \tag{32}$$

It is worth mentioning that, a total of 10,000 samples are generated through the *Monte Carlo* simulation, where the values of $\mathrm{Biomass}_{m,t}^{\mathrm{AVAILABLE}}$, $F_{m,t}^{\mathrm{OIL\_DEMAND}}$, $C_{m,t}^{\mathrm{BIOMASS}}$, $C_{m,t}^{\mathrm{COAL}}$, $C_{m,t}^{\mathrm{FUEL}}$, $C_{m,t}^{\mathrm{OIL}}$ and $MC_{m,t}^{\mathrm{IN}}$ for each sample is randomized based on the statistical data. With this, the supply uncertainty, demand variation, price fluctuation, and seasonal biomass quality can, therefore, be incorporated into the model. The NPV and PBP (determined *via* subtraction method) of these samples are determined. Subsequently, the effectiveness of the proposed action plans is evaluated based on the improvement of these two economic indicators.

4.2 Illustrative Example

An oil palm biomass-based polygeneration plant is used as an illustrative case study to demonstrate how *Monte Carlo* simulation can be used to aid the policy selection decision. Empty fruit bunch (EFB) is collected from a nearby palm oil mill (located 10 km away from the plant). They are subsequently dried before feeding into the pyrolyser in the polygeneration plant. The produced bio-oil can be sold to a demand point which is located 15 km away from the plant, while the syngas and biochar are used as energy sources for power and thermal energy. The energy can be self-consumed so that the requirement of an external energy source can be mitigated. As mentioned in Sect. 4.2, the excess generated electricity can be exported to grid for additional revenue. The visual illustration of this case study is presented in Fig. 7, while all the important parameters used to develop the case study model are summarised in Tables 10 and 11. As mentioned, the fluctuations and uncertainties in operations, transportation, market demand, and price can be rigorously modeled by *Monte Carlo* simulations based on the actual statistical distributions. Figure 8 shows the 10,000 sample points generated based on the statistical data stated in Table 10 (i.e., the mean (μ) and standard deviation (σ)) for each randomized parameter. By judging on the frequency of the data points, one can estimate the occurrence probability of the parameters' magnitude. Taking biomass moisture content (Fig. 7b) as an example, the probability of getting a moisture content of less than 70% during the rainy season is significantly lower as compared to that of the dry season. In terms of EFB availability, 8500–11,000 t EFB/month, 11,000–12,400 t EFB/month, and 12,800–15,000 t EFB/month are available in low season, mid season, and the high season, respectively (Fig. 8a, b). Whereas the price fluctuations for EFB (24.55–73.65 USD/t), coal (24.55–147.30 USD/t), oil (0.74–0.88 USD/L), and diesel (0.44–0.60 USD/L) are shown in Fig. 8a, c. Aside from that Fig. 8d presents the oil demand variation, where the peak is found in the middle of the year (around June), and declines from December to February. Table 12, on the other hand, presents the description and the explanation of the seven action plans. To indicate the implementation of each action plan, the model settings stated in Table 12 were conducted (e.g., to represent the implementation of AP5, the TAX is omitted in the first five years.

Figure 9 shows the *Monte Carlo* simulation results obtained under different action plans. As shown in Fig. 9a, it is observed that introducing a new financing incentive (AP3-FI) attains the most attractive result, i.e., leading to a 58.51% (equivalent to ~ 1.6×10^6 USD) increment in the mean of NPV as compared to the base case (without

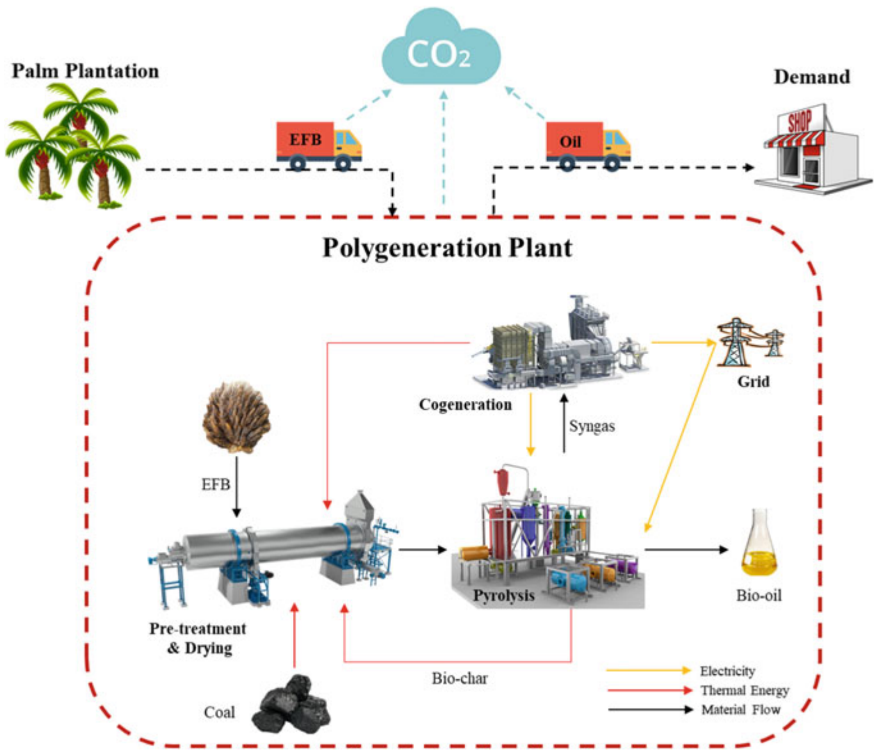

Fig. 7 Schematic diagram of the polygeneration plant case study (Ngan et al., 2020)

Table 10 Randomized parameters used for this case study (adapted from Ngan et al., 2020)

Parameter	Remark	Value	Reference
$\text{Biomass}_{m,t}^{\text{AVAILABLE}}$(t/month)	Low Season[a] Mid Season[a] High Season[a]	$\mu = 9890.82; \sigma = 323.69$ $\mu = 11{,}664.92; \sigma = 203.37$ $\mu = 13{,}853.1; \sigma = 350.30$	Malaysian Palm Oil Board (MPOB) (2018)
$F_{m,t}^{\text{OIL\_DEMAND}}$(t/month)	January[b] February[b] March[b] April[b] May[b] June[b] July[b] August[b] September October[b] November[b] December[b]	$\mu = 918.60; \sigma = 90.86$ $\mu = 915.60; \sigma = 65.80$ $\mu = 926.70; \sigma = 82.86$ $\mu = 927.75; \sigma = 69.03$ $\mu = 960.00; \sigma = 66.95$ $\mu = 957.45; \sigma = 48.72$ $\mu = 984.27; \sigma = 63.89$ $\mu = 978.95; \sigma = 59.60$ $\mu = 970.77; \sigma = 61.26$ $\mu = 936.82; \sigma = 68.21$ $\mu = 929.18; \sigma = 92.27$ $\mu = 924.95; \sigma = 89.10$	Trading Economics (2018)
$\boldsymbol{C_{m,t}^{\textbf{BIOMASS}}}$(USD/t)	–	Max = 34.18; Min = 70.80	-
$\boldsymbol{C_{m,t}}^{\text{COAL}}$(USD/t)	–	$\mu = 70.26; \sigma = 19.43$	Index Mundi (2018)
$\boldsymbol{C_{m,t}}^{\text{FUEL}}$(USD/L)	–	$\mu = 0.52; \sigma = 0.03$	RinggitPlus (2018)
$\boldsymbol{C_{m,t}}^{\text{OIL}}$(USD/L)	–	$\mu = 0.82; \sigma = 0.03$	–
$\text{MC}_{\boldsymbol{m,t}}^{\text{IN}}$(%)	Dry season Rainy season[c]	$\mu = 66.5; \sigma = 1.83$ $\mu = 76.5; \sigma = 1.83$	International Finance Corporation (IFC) (2017)

[a] Classified based on the monthly palm crude oil production (Andiappan et al., 2015)
[b] The local bio-oil demand is assumed similar to the pattern of the oil production in Malaysia
[c] Assumed to be 10% greater than that of during dry season

Table 11 Fixed parameters used for this case study (adapted from Ngan et al., 2020)

Parameter	Remark	Value	Reference
$MC_{m,t}^{OUT}(\%)$	–	10	–
$y^{OIL}(\%)$	–	27	Mohd (2017)
$y^{GAS}(\%)$	–	24	Mohd (2017)
$y^{CHAR}(\%)$	–	49	Mohd (2017)
$y_g^{PY}(\%)$	H_2 CO CH_4 CO_2	3.7 34.0 7.8 54.0	Mohd (2017)
$y^{CO_2\_TR}$(kg CO_2/L fuel)	–	2.68	Gu and Bergman (2015)
$y^{CO_2\_COGEN}$(kg CO_2/kWh)	–	0.525	Gu and Bergman (2015)
LHV_g(kJ/mol)	H_2 CO CH_4	240.2 283.5 801.4	PNAS (2018)
LHV^{COAL}(MJ/kg)	–	23	Othman et al. (2012)
LHV^{CHAR}(MJ/kg)	–	26	Mohamad et al. (2011)
$\xi^{COGEN}(\%)$	–	27[a]	–
$\xi^{DRY}(\%)$	–	85	–
ψ^{PY}(kWh/t EFB)	–	240	Rogers and Brammer (2012)
ψ^{FUEL}(L fuel/km)	–	0.213	How et al. (2016)
$\psi^{THERMAL}$(MJ/kg water removed)	–	4	Kovařík (2017)
TAX(%)	–	24	–
in(%)	–	10	–
C_u^{CAPEX}(M USD)	Pyrolyser Co-generation	1.54[b] 0.48	Wright et al. (2010), Energy Technology Systems Analysis Programme (ETSAP) (2010)
$C_{u,m,t}^{OPEX}$(USD/unit[c])	Pyrolyser Co-generation	50 60	How and Lam (2018) –
C^{FIT}(USD/kWh)	–	0.12	Sustainable Energy Development Authority Malaysia (SEDA) (2018)
C^{ELEC}(USD/kWh)	–	0.14	–
C^{CO_2}(USD/kg CO_2)	–	0.05	How et al. (2016)
Cap^{TRUCK}	–	10	–
d^S(km/trip)	–	10	–
d^D(km/trip)	–	15	–

[a] Assumed to be 60% of the typical gas engine efficiency
[b] Scaled by using six-tenths rule
[c] USD/t EFB for pyrolyser; USD/MWh for co-generation unit

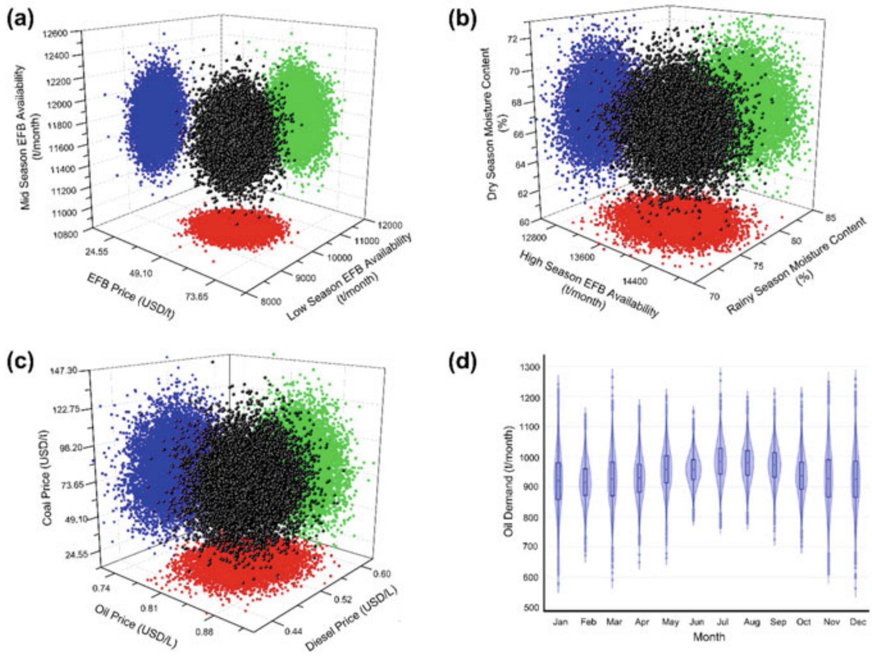

Fig. 8 Randomized input for: **a** Mid and high season EFB availability, EFB price; **b** dry and rainy season moisture content, low season EFB availability; **c** coal price, oil price, and diesel price, **d** oil demand (Ngan et al., 2020)

any action plan). On the other hand, as shown in Fig. 9c, PBP is also improved by 12.22% (equivalent to 7 months). Figure 9b shows that this action plan is capable to offer a maximum NPV of 6.14 million USD in 20 years, which is about 1.3 times greater than the next highest action plan (i.e., AP6-RF). Nevertheless, AP3-FI has demonstrated a mean PBP of 4 years which is the second shortest PBP among all action plans (Fig. 9c, d). Whereas the next most convincing action plan is to revise Fit-in-Tariff (AP6-RF) which has an expected NPV of between 2.9 and 3.4 million USD in 20 years and a mean PBP of 4 years. In other words, by adopting this action plan (increase the FiT rates to 0.132 USD/kWh), the overall NPV can be increased by 20.72% with a 14.04% reduction in PBP. In fact, multiple countries have achieved successful growth in renewable energy sectors through the implementation of FiT (e.g., Thailand has successfully increased the power generation capacity by renewable sources from 8% in 2015 to 17% by the end of 2017 with an attractive FiT rate (International Renewable Energy Agency (IRENA) 2017).

The action plan that ranked 3rd is AP5-TI (introducing tax incentives). Identical to financing incentives, the tax incentive is another type of financial instrument that is widely used by the government to spur up the growth of an industry. Some of the examples of tax incentives are tax returns, tax exemption, and tax reduction. The simulation result for implementing AP5-TI enhances the mean of the NPV by

Table 12 Description for each action plant (adapted from Ngan et al., 2020)

ID	Action plan	Description	Model setting
AP1-HD	Engage in demand contract	To hedge demand risk by committed into a supply contract with the consumer(s), to sell a fixed amount of product for a fixed duration, with a fixed price that is lower than that of the current market price	Set contracted demand as 1700 t/year $C_{m,t}^{\mathrm{OIL}}$ is set 3% lesser than the current market price
AP2-HS	Engage in supply contract	To hedge supply risk by committed into a purchase contract with supplier(s), to buy a fixed amount of raw materials for a fixed duration, with a fixed price that greater than that of the current market price	St contracted supply as 10,000 t/year $C_{m,t}^{\mathrm{BIOMASS}}$ is set 10% higher than the current market price
AP3-FI	Introduce new financing incentive	To reduce financing risk by providing financing incentives in the form of interest rate reduction to lower the debt obligation of industry players	Set in as 6%
AP4-SF	Substitute fossil fuel with biodiesel	To encourage the substitution of conventional fossil fuel which is less environmentally friendly with biodiesel to mitigate the overall CO_2 emissions	Set $C_{m,t}^{\mathrm{FUEL}}$ as 0.69 USD/L and $y^{\mathrm{CO_2\_TR}}$ as 2.1 kg CO_2/L
AP5-TI	Introduce new tax incentive	To reduce regulatory risk by showing favor in the form of tax exemption to encourage the utilization of biomass for wealth generation and development of green industry	Set TAX as 0% for the first 5 years
AP6-RF	Revise Feed-in-Tariff (FiT) rate	To promote higher utilization of renewable energy by revising the FiT rate to a higher rate to make it attractive for new entrants and investors to venture into the industry	Increase C^{FIT} by 10%

(continued)

Table 12 (continued)

ID	Action plan	Description	Model setting
AP7-CM	Introduce carbon management system	To promote sustainable development by introducing carbon management system upfront to avoid high carbon emission which could potentially result in carbon penalty	Set the removal efficiency as 80%[a]

[a] Assumed the total CAPEX to be 60% more expensive (Ooi et al., 2014) while the OPEX of the carbon management system is set as 0.037 USD/kg CO_2 removed (Rubin et al., 2015)

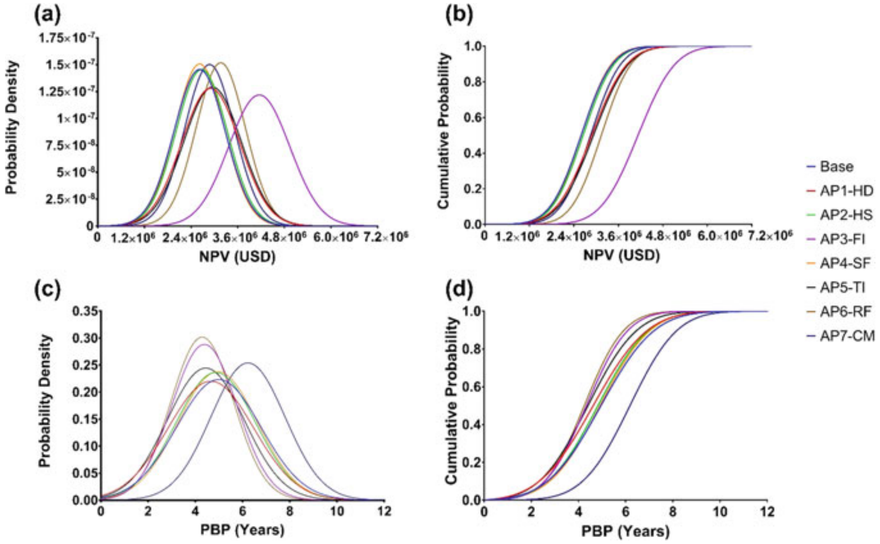

Fig. 9 The effect of the respective action plans on NPV (**a** probability density; **b** Cumulative probability) and PBP (**c** probability density; **d** cumulative probability) from 10,000 *Monte Carlo* simulations (Ngan et al., 2020)

12.62% (equivalent to ~ 0.34 × 10^6 USD), and reducing the payback period by 11.04% (equivalent to 6 months). It is followed by AP1-HD and AP2-HS which aim to mitigate the risks associated with the potential fluctuations in biomass supply and the product demand. It is a common strategy opted in the industry for production plants to engage in a long-term supply or/and demand contract to supply or purchase a fixed quantity of the product at a fixed price, for a fixed duration. The increase of mean of NPV for AP1-HD and AP2-HS is 10.84% (equivalent to ~ 0.3 × 10^6 USD) and 1.95% (equivalent to ~ 0.5 × 10^5 USD) respectively, while the mean PBP for each action plan is 6.68% (equivalent to 4 months) and 2.49% (equivalent to 1 month) respectively. It is worthfully to note that the combination of both action plans can yield better economic performance, i.e., 15.31% in terms of NPV improvement (equivalent to ~ 0.4×10^6 USD) and 9.46% in terms of PBP improvement equivalent to 5 months), which is comparable to AP5-TI.

Introduce carbon management system (AP7-CM) and substitute fossil fuel with biodiesel (AP4-SF) are ranked at the least. Both of these action plans aim to improve the overall economic performance *via* the mitigation of carbon emissions. Despite a significant increment (9.69% or equivalent to ~ 0.26×10^6 USD) of NPV are spotted for AP7-CM, the additional CAPEX required for the carbon capture system has prolonged the duration of PBP by 24.75% (equivalent to 2 years of additional project time). This shows that the uptake of CCS at this stage is categorized as a high-risk decision and not so favorable as compared to other action plans which could achieve a similar improvement in NPV, without the need to incur a higher upfront cost. Nevertheless, this finding is by no means an unchangeable fact as the incurred costs can be possibly reduced substantially as the technology matures (Mott MacDonald, 2012). Lastly, AP4-SF has shown a very minimal impact on both the NPV and PBP. This is due to the insignificant carbon penalty reduction (i.e., reduced about 0.03 USD/L) which is unable to compensate for the greater fuel cost (i.e., increased about 0.17 USD/L).

5 Further Reading

The following listed materials are recommended for further reading:

(i) Overview of sustainable biomass supply chain: from concept to modeling (Hong et al., 2016)

This paper provides readers with the fundamental knowledge and concept of sustainable biomass supply chain management, modeling, and optimization. In addition, key challenges and future prospects were elucidated comprehensively in this review article.

(ii) PCA method for debottlenecking of sustainability performance in integrated biomass supply chain (How & Lam, 2019)

This paper proposes a novel principal component analysis (PCA) aided debottlenecking approach to systematically remove the potential sustainability bottlenecks. Its effectiveness is benchmarked with another graph-theoretic based debottlenecking approach.

(iii) Techno-economic analysis for biomass supply chain: A state-of-the-art review (Lo et al., 2021)

This paper critically reviews the available approaches for the techno-economic evaluation of biomass supply chain (deterministic and stochastic). In addition, this review article outlines the key supply chain uncertainties and their corresponding impacts on the economic performance of the biomass business.

(iv) Debottlenecking of biomass element deficiency in a multiperiod supply chain system *via* element targeting approach (Lim et al., 2019)

This paper tackles the biomass availability fluctuation in a given regional biomass supply chain using element targeting approach and multiperiod analysis. This article demonstrates how the element targeting approach can be used to improve the overall biomass resources allocation and utilization.

(v) Synthesis of sustainable circular economy in palm oil industry using graph-theoretic method (Yeo et al., 2020)

This paper attempts to evaluate the feasibility of shifting the conventional palm oil industry toward circular economy using a powerful graph-theoretic approach, called process graph (P-graph). The potential bottlenecks that hinder the implementation of circular economy approach have also been discussed.

(vi) Bottleneck Tree Analysis (BOTA) with green and lean index for process capacity debottlenecking in industrial refineries (Teng et al., 2020)

This paper proposes a novel Bottleneck Tree Analysis (BOTA) to optimize the debottlenecking schedule in industrial refineries with the consideration of lean and green aspects. Such an effective scheduling approach can be easily adapted in palm oil refinery and biorefinery.

6 Conclusion

Palm biomass supply chain is deemed as a waste-to-wealth business. It contributes to economic development and serves as an effective strategy for waste management. Nevertheless, the complete shift to biomass as a feedstock is yet to be proven feasible and sustainable at a commercial scale. To fully explore its real potential and limits, sufficient knowledge and in-depth understanding of biomass supply chain modeling, particularly in stochastic modeling are essentially needed. This chapter, therefore, provides an overview of the key factors to be considered in stochastic modeling for biomass supply chain. It serves as a general guide to industry practitioners, academicians, and researchers who have interest in equipping themselves with knowledge and skills regarding stochastic modeling of the biomass supply chain. Three illustrative examples are used to demonstrate the utility of stochastic modeling in biomass supply chain research (i.e., biomass selection decision, facilities location decision, and policy selection decision). All these contents will help readers to understand stochastic biomass supply chain modeling from a wider perspective before venturing into this waste-to-wealth business.

Acknowledgements The author would like to acknowledge the financial support from the Ministry of Higher Education under the Fundamental Research Grant Scheme [grant number: FRGS/1/2020/TK0/SWIN/03/3] and Swinburne University of Technology Sarawak *via* Research Supervision Grant [grant number: 2-5545 RSG].

References

Abas, R., Kamarudin, M. F., Nordin, A. B. A., & Simeh, M. A. (2011). A study on the Malaysian oil palm biomass sector—supply and perception of palm oil millers. *Oil Palm Industry Economic Journal, 11*, 28–41.
Aboytes-Ojeda, M., Castillo-Villar, K. K., & Eksioglu, S. D. (2019). Modeling and optimization of biomass quality variability for decision support systems in biomass supply chains. *Annals of Operations Research, 314*, 319–346.
Agensi Inovasi Malaysia. National Biomass Strategy 2020: New wealth creation for Malaysia's biomass industry 2013.
Aghabararnejad, M, Patience, G. S., & Chaouki, J. (2015). Techno-economic comparison of a 7-mwth biomass chemical looping gasification unit with conventional systems. *Chemical Engineering & Technology, 38*(5), 867–878.
Ahmad, R., Hamidin, N., Md Ali, U., & Abidin, C. Z. A. (2014). Characterization of bio-oil from palm kernel shell pyrolysis. *Journal of Mechanical Engineering and Sciences., 7*, 1134–1140.
Ahmad, S., Ab Kadir, M. Z. A., & Shafie, A. S. (2011). Current perspective of the renewable energy development in Malaysia. *Renewable and Sustainable Energy Reviews, 15*(2), 897–904.
AlNouss, A., Parthasarathy, P., Shahbaz, M., Al-Ansari, T., Mackey, H., & McKay, G. (2020). Techno-economic and sensitivity analysis of coconut coir pith-biomass gasification using ASPEN PLUS. *Applied Energy, 261*, 114350.
Andiappan, V., Tan, R. R., Aviso, K. B., & Ng, D. K. S. (2015). Synthesis and optimisation of biomass-based tri-generation systems with reliability aspects. *Energy, 89*, 803–818.
Aziz, M.A., Uemura, Y., & Sabil, K.M. (2011). Characterization of oil palm biomass as feed for torrefaction process. In *2011 National Postgraduate Conference* (pp. 1–6).
Baral, N. R., Davis, R., & Bradley, T. H. (2019). Supply and value chain analysis of mixed biomass feedstock supply system for lignocellulosic sugar production. *Biofuel Bioprod Bior, 13*(3), 635–659.
Barde, S. R. A., Yacout, S., & Shin, H. (2019). Optimal preventive maintenance policy based on reinforcement learning of a fleet of military trucks. *Journal of Intelligent Manufacturing, 30*, 147–161.
Bussemaker, M. J., Day, K., Drage, G., & Cecelja, F. (2017). Supply chain optimisation for an ultrasound-organosolv lignocellulosic biorefinery: Impact of technology choices. *Waste Biomass Valori, 8*, 2247–2261.
Chou, J.-S., & Ongkowijoyo, C. S. (2014). Risk-based group decision making regarding renewable energy schemes using a stochastic graphical matrix model. *Automation in Construction, 37*, 98–109.
Department of Statistic Malaysia. (2020). Selected agricultural indicators, Malaysia, 2020. DOSM. [Online] Available at www.dosm.gov.my. Accessed March 1, 2021.
DQS Certification. MSPO Certification Summary Report 2018. https://www.dqs.com.my/wp-content/uploads/2019/07/SOPB_Galasah-Palm-Oil-Mill_2018-AA3_Report.pdf. Accessed April 7, 2021.
Energy Information Administration (EIA). 2021. Country Analysis Executive Summary: Malaysia. [Online] Available at https://www.eia.gov/international/content/analysis/countries_long/Malaysia/malaysia.pdf. Accessed March 26, 2021.
Energy Technology Systems Analysis Programme (ETSAP). 2010. Combined heat and power. Available at www.etsap.org. Accessed March 6, 2021.
Garba, K., Mohd Din, A.T., & Hameed, B. (2017). Pyrolysis of oil palm mesocarp fiber and palm frond in a slow-heating fixed-bed reactor: A comparative study. *Bioresource Technology, 241*.
GE. (2018). Jenbacher gas engines. [Online] Available at http://kts-eng.com/assets/files/J208.pdf. Accessed February 1, 2021.
Gu, H., & Bergman, R. (2015). Life-cycle GHG emissions of electricity from syngas produced by pyrolyzing woody biomass. In *Proceedings of the 58th International Convention of Society*

of Wood Science and Technology June 7–12, 2015. Jackson Lake Lodge, Grand Teton National Park, Wyoming, U.S.A.

Han, J., Liang, Y., Hu, J., Qin, L., Street, J., Lu, Y., & Yu, F. (2017). Modeling downdraft biomass gasification process by restricting chemical reaction equilibrium with Aspen Plus. *Energy Conversion and Management, 153*, 641–648.

Hong, B. H., How, B. S., & Lam, H. L. (2016). Overview of sustainable biomass supply chain: From concept to modelling. *Clean Technologies and Environmental Policy, 18*, 2173–2194.

How, B. S., & Lam, H. L. (2018). Sustainability evaluation for biomass supply chain synthesis: Novel principal component analysis (PCA) aided optimisation approach. *Journal of Cleaner Production, 189*, 941–961.

How, B. S., & Lam, H. L. (2019). PCA method for debottlenecking of sustainability performance in integrated biomass supply chain. *Process Integration and Optimization for Sustainability, 3*, 43–64.

How, B. S., Ngan, S. L., Hong, B. H., Lam, H. L., Ng, W. P. Q., Yusup, S., et al. (2019). An outlook of Malaysian biomass industry commercialisation: Perspectives and challenges. *Renewable and Sustainable Energy Reviews, 113*, 109277.

How B.S., Tan K.Y., & Lam H.L. (2016). Transportation decision tool for optimisation of integrated biomass flow with vehicle capacity constraints. *Journal of Cleaner Production, 136* (Part B), 197–223.

International Energy Agency (IEA). (2019). Renewable energy. [Online] Available at https://www.iea.org/policiesandmeasures/renewableenergy/?country=Malaysia. Accessed March 20, 2021.

International Finance Corporation (IFC). (2017). *Converting biomass to energy: A guide developers and investors*. International Finance Corporation.

Index Mundi. (2018). Coal, Australian thermal coal monthly price—Malaysian Ringgit per Metric Ton. [Online] Available at www.indexmundi.com. Accessed January 10, 2021.

International Renewable Energy Agency (IRENA). (2017). Renewable energy outlook: Thailand, international renewable energy agency, Abu Dhabi. [Online] Available at www.irena.org. Accessed January 3, 2021.

Khatiwada, D., Leduc, S., Silveira, S., & McCallum, I. (2016). Optimizing ethanol and bioelectricity production in sugarcane biorefineries in Brazil. *Renewable Energy, 85*, 371–386.

Kieffer, M., Brown, T., & Brown, R. C. (2016). Flex fuel polygeneration: Integrating renewable natural gas into fischer-tropsch synthesis. *Applied Energy, 170*, 208–218.

Kovařík, P. (2017). *Drying of biomass with high water content (Master Thesis)*. Czech Technical University, Prague.

Kristianto, Y., & Zhu, L. D. (2017). Techno-economic optimization of ethanol synthesis from rice-straw supply chain. *Energy, 141*, 2164–2176.

Lam, H. L., Ng, W. P. Q., Ng, R. T. L., Ng, E. H., Aziz, M. K. A., & Ng, D. K. S. (2013). Green strategy for sustainable waste-to-energy supply chain. *Energy, 57*, 4–16.

Lembaga Hasil Dalam Negeri Malaysia (LHDN). (2018). Investment tax allowance. LHDN. [Online] Available at www.hasil.gov.my. Accessed February 1, 2021.

Lim, C. H., How, B. S., Ng, W. P. Q., & Lam, H. L. (2019). Debottlenecking of biomass element deficiency in a multiperiod supply chain system via element targeting approach. *Journal of Cleaner Production, 230*, 751–766.

Lin, J. F., Gaustad, G., & Trabold, T. A. (2013). Profit and policy implications of producing biodiesel-ethanol-diesel fuel blends to specifications. *Applied Energy, 104*, 936–944.

Lo, S. L. Y., How, B. S., Leong, W. D., Teng, S. Y., Rhamdhani, M. A., & Sunarso, J. (2021). Techno-economic analysis for biomass supply chain: A state-of-the-art review. *Renewable and Sustainable Energy Reviews, 135*, 110164.

Lo, S. L. Y., Choo, J. J. L., Kong, K. G. H., How, B. S., Lam, H. L., Ngan, S. L., Lim, C. H., & Sunarso, J. (2020). Uncertainty study of empty fruit bunches-based bioethanol supply chain. *Chemical Engineering Transactions, 81*, 601–606.

Mahlia, T. M. I., Abdulmuin, M. Z., Alamsyah, T. M. I., & Mukhlishien, D. (2001). An alternative energy source from palm wastes industry for Malaysia and Indonesia. *Energy Conversion and Management, 42*, 2109–2118.

Malaysian Palm Oil Board (MPOB). (2018). Production of crude palm oil for the month of December 2017. [Online] Available at bepi.mpob.gov.my. Accessed January 10, 2021.

MarketsandMarkets Research Private Ltd. (2021). Syngas & derivatives market by production technology, gasifier type, feedstock (coal, natural gas, petroleum byproducts, biomass/waste), application (chemicals, fuel, and electricity), and region—global forecast to 2025. [Online] Available at https://www.marketsandmarkets.com/Market-Reports/syngas-market-1178.html. Accessed March 10, 2021.

Martinkus, N., Latta, G., Brandt, K., & Wolcott, M. (2018). A multi-criteria decision analysis approach to facility siting in a wood-based depot-and-biorefinery supply chain model. *Front Energy Res, 6*, 124.

Mohamad, A. S., Loh, S. K., Nasrin, A. B., & Choo, Y. M. (2011). Production and characterization of bio-char from the pyrolysis of empty fruit bunches. *American Journal of Applied Sciences, 8*(10), 984–988.

Mohd N.A. (2017). *Conventional and microwave pyrolysis of empty fruit bunch and rice husk pellets*. Ph.D. Thesis, The University of Sheffield, Sheffield, U.K.

Monthly Production of Oil Palm Products Summary 2019 & 2020. Malaysia Palm Oil Board. (2020). http://bepi.mpob.gov.my/index.php/en/production/production-2020/production-of-oil-palm-products-2020.html. Accessed March 26, 2021

MacDonald, M. (2012). Potential cost reductions in CCS in the power sector. Department of Energy and Climate Change, Mott Mac Donald, London, U.K.

Ngan, S. L., How, B. S., Teng, S. Y., Leong, W. D., Loy, A. C. M., Yatim, P., Promentilla, M. A. B., & Lam, H. L. (2020). A hybrid approach to prioritize risk mitigation strategies for biomass polygeneration systems. *Renewable and Sustainable Energy Reviews, 121*, 109679.

Ooi, R. E. H., Foo, D. C. Y., & Tan, R. R. (2014). Targeting for carbon sequestration retrofit planning in the power generation sector for multi-period problems. *Applied Energy, 113*, 477–487.

Othman N.F., Boosroh M.H., Hassan H., Mohan C., & Aziz W.A.L.W.A. (2012). Gasification of triple fuel blends using pilot scale fluidized bed gasification plant. In *Proceeding of International Conference on Science, Technology & Social Sciences (ICSTSS)* (pp. 471–477).

PNAS. (2018). SI appendix general information and assumption. [Online] Pnas.org. Available at http://www.pnas.org. Accessed March 6, 2021.

Reduan, H. (2017). FGv unit to export 60,000 tonnes of palm kernel shells to Japan. *New Straits Time*.

RinggitPlus. (2018). Petrol price Malaysia live updates (RON95, RON97 & Diesel). [Online] Available at ringgitplus.com. Accessed January 10, 2021.

Rogers, J. G., & Brammer, J. G. (2012). Estimation of the production cost of fast pyrolysis bio-oil. *Biomass and Bioenergy, 36*, 208–217.

Rubin, E. S., Davison, J. E., & Herzog, H. J. (2015). The cost of CO_2 capture and storage. *International Journal of Greenhouse Gas Control, 40*, 378–400.

Shou, Z., Di, X., Ye, J., Zhu, H., Zhang, H., & Hampshire, R. (2020). Optimal passenger-seeking policies on E-hailing platforms using Markov decision process and imitation learning. *Transportation Research Part c: Emerging Technologies, 111*, 91–113.

Sohni, S., Norulaini, N. A. N., Hashim, R., Khan, S. B., Fadhullah, W., & Mohd Omar, A. K. (2018). Physicochemical characterization of Malaysian crop and agro-industrial biomass residues as renewable energy resources. *Industrial Crops and Products, 111*, 642–650.

Song, G., Feng, F., Xiao, J., & Shen, L. (2013). Technical assessment of synthetic natural gas (SNG) production from agriculture residuals. *Journal of Thermal Science, 22*, 359–365.

Spath, P., Aden, A., Eggeman, T., Ringer, M., Wallace, B., & Jechura, J. (2005). Biomass to hydrogen production detailed design and economics utilizing the battelle columbus laboratory indirectly-heated gasifier. [Online] Available at https://www.nrel.gov/docs/fy05osti/37408.pdf. Accessed November 30, 2020.

StatEase. ANOVA Output. StatEase; 2020.
Susanto, H., Suria, T., & Pranolo, S. H. (2018). Economic analysis of biomass gasification for generating electricity in rural areas in Indonesia. *IOP Conference Series: Materials Science and Engineering , 334*, 012012.
Sustainable Energy Development Authority Malaysia (SEDA). (2018). FiT rates for biomass (solid waste) (16 years from FiT commencement date). Available at www.seda.gov.my/. Accessed March 6, 2021.
Tanzer, S. E., Posada, J., Geraedts, S., & Ramírez, A. (2019). Lignocellulosic marine biofuel: Technoeconomic and environmental assessment for production in Brazil and Sweden. *Journal of Cleaner Production, 239*, 117845.
Teng, S. Y., How, B. S., Leong, W. D., Teoh, J. H., Cheah, A. C. S., Motavasel, Z., & Lam, H. L. (2019). Principal component analysis-aided statistical process optimisation (PASPO) for process improvement in industrial refineries. *Journal of Cleaner Production, 225*, 359–375.
Teng, S. Y., How, B. S., Leong, W. D., Teoh, J. H., & Lam, H. L. (2020). Bottleneck Tree Analysis (BOTA) with green and lean index for process capacity debottlenecking in industrial refineries. *Chemical Engineering Science, 214*, 115429.
The Oil Palm. History of the Industry. (2021). [Online] Available at http://theoilpalm.org/about/#History_and_Origin. Accessed March 25, 2021
Trading Economics. (2018). Commodity crude oil. [Online] Available at www.tradingeconomics.com. Accessed January 10, 2021.
Trading Economics. (2020). Malaysia gasoline price. [Online] Available at https://tradingeconomics.com/malaysia/gasoline-prices. Accessed March 20, 2021.
Wang, S., Levin, M. W., & Caverly, R. J. (2021). Optimal parking management of connected autonomous vehicles: A control-theoretic approach. *Transportation Research Part c: Emerging Technologies, 124*, 102924.
Wright, M. M., Satrio, J. A., Brown, R. C., Daugaard, D. E., & Hsu, D. D. (2010). *Techno-economic analysis of biomass fast pyrolysis to transportation fuels*. National Renewable Energy Laboratory (NREL), Colorado, U.S.A.
Yatim, P., Mamat, M. N., Mohamad-Zailani, S. H., & Ramlee, S. (2016). Energy policy shifts towards sustainable energy future for Malaysia. *Clean Technology Environment Policy, 18*, 1685–1695.
Yeo, J. Y. J., How, B. S., Teng, S. Y., Leong, W. D., Ng, W. P. Q., Lim, C. H., Ngan, S. L., Sunarso, J., & Lam, H. L. (2020). Synthesis of sustainable circular economy in palm oil industry using graph-theoretic method. *Sustainability, 12*, 8081.
Yoo, H.-M., Park, S.-W., Seo, Y.-C., & Kim, K.-H. (2019). Applicability assessment of empty fruit bunches from palm oil mills for use as bio-solid refuse fuels. *Journal of Environmental Management, 234*, 1–7.
Zakaria, A., Ismail, F. B., Hossain Lipu, M. S., & Hannan, M. A. (2020). Uncertainty models for stochastic optimization in renewable energy applications. *Renewable Energy, 145*, 1543–1571.
Zuldian, P., Fukuda, S., & Bustan, M. (2017). Economic analysis of coal gasification plant for electricity and thermal energy supplies in Indonesia. *Journal of Clean Energy Technologies, 5*, 193–198.